17 Zhang H, Zhang N, Li M et al. Therapeutic angiogenesis of bone marrow mononuclear cells (MNCs) and peripheral blood MNCs: Transplantation for ischemic hindlimb. Ann Vasc Surg 2008;22:238–247.
18 Tse HF, Kwong YL, Chan JK et al. Angiogenesis in ischaemic myocardium by intramyocardial autologous bone marrow mononuclear cell implantation. Lancet 2003;361:47–49.
19 Kamihata H, Matsubara H, Nishiue T et al. Implantation of bone marrow mononuclear cells into ischemic myocardium enhances collateral perfusion and regional function via side supply of angioblasts, angiogenic ligands, and cytokines. Circulation 2001;104:1046–1052.
20 Wang QR, Wang BH, Huang YH et al. Purification and growth of endothelial progenitor cells from murine bone marrow mononuclear cells. J Cell Biochem 2008;103:21–29.
21 Kawamoto A, Losordo DW. Endothelial progenitor cells for cardiovascular regeneration. Trends Cardiovasc Med 2008;18:33–37.
22 Kim H, Park JS, Choi YJ et al. Bone marrow mononuclear cells have neurovascular tropism and improve diabetic neuropathy. Stem Cells 2009;27:1686–1696.
23 Sheikh AY, Lin SA, Cao F et al. Molecular imaging of bone marrow mononuclear cell homing and engraftment in ischemic myocardium. Stem Cells 2007;25:2677–2684.
24 Pittenger MF, Mackay AM, Beck SC et al. Multilineage potential of adult human mesenchymal stem cells. Science 1999;284:143–147.
25 Brenneman M, Sharma S, Harting M et al. Autologous bone marrow mononuclear cells enhance recovery after acute ischemic stroke in young and middle-aged rats. J Cereb Blood Flow Metab 2010;30: 140–149.
26 Chen J, Zhang ZG, Li Y et al. Intravenous administration of human bone marrow stromal cells induces angiogenesis in the ischemic boundary zone after stroke in rats. Circ Res 2003;92:692–699.
27 Li Y, Chen J, Chen XG et al. Human marrow stromal cell therapy for stroke in rat: Neurotrophins and functional recovery. Neurology 2002; 59:514–523.
28 Chen J, Li Y, Wang L et al. Therapeutic benefit of intracerebral transplantation of bone marrow stromal cells after cerebral ischemia in rats. J Neurol Sci 2001;189:49–57.
29 Honma T, Honmou O, Iihoshi S et al. Intravenous infusion of immortalized human mesenchymal stem cells protects against injury in a cerebral ischemia model in adult rat. Exp Neurol 2006;199:56–66.
30 Iihoshi S, Honmou O, Houkin K et al. A therapeutic window for intravenous administration of autologous bone marrow after cerebral ischemia in adult rats. Brain Res 2004;1007:1–9.
31 Kamiya N, Ueda M, Igarashi H et al. Intra-arterial transplantation of bone marrow mononuclear cells immediately after reperfusion decreases brain injury after focal ischemia in rats. Life Sci 2008;83:433–437.
32 Giraldi-Guimaraes A, Rezende-Lima M, Bruno FP et al. Treatment with bone marrow mononuclear cells induces functional recovery and decreases neurodegeneration after sensorimotor cortical ischemia in rats. Brain Res 2009;1266:108–120.
33 Taguchi A, Soma T, Tanaka H et al. Administration of CD34+ cells after stroke enhances neurogenesis via angiogenesis in a mouse model. J Clin Invest 2004;114:330–338.
34 Taguchi A, Wen Z, Myojin K et al. Granulocyte colony-stimulating factor has a negative effect on stroke outcome in a murine model. Eur J Neurosci 2007;26:126–133.
35 Okabe M, Ikawa M, Kominami K et al. 'Green mice' as a source of ubiquitous green cells. FEBS Lett 1997;407:313–319.
36 Iwai M, Liu HW, Chen R et al. Possible inhibition of focal cerebral ischemia by angiotensin II type 2 receptor stimulation. Circulation 2004;110:843–848.
37 Lendahl U, Zimmerman LB, McKay RD. CNS stem cells express a new class of intermediate filament protein. Cell 1990;60:585–595.
38 Gravdal K, Halvorsen OJ, Haukaas SA et al. Proliferation of immature tumor vessels is a novel marker of clinical progression in prostate cancer. Cancer Res 2009;69:4708–4715.
39 Reynolds BA, Weiss S. Generation of neurons and astrocytes from isolated cells of the adult mammalian central nervous system. Science 1992;255:1707–1710.
40 Ellis P, Fagan BM, Magness ST et al. SOX2, a persistent marker for multipotential neural stem cells derived from embryonic stem cells, the embryo or the adult. Dev Neurosci 2004;26:148–165.
41 Schwarting S, Litwak S, Hao W et al. Hematopoietic stem cells reduce postischemic inflammation and ameliorate ischemic brain injury. Stroke 2008;39:2867–2875.
42 Okada S, Nakauchi H, Nagayoshi K et al. In vivo and in vitro stem cell function of c-kit- and Sca-1-positive murine hematopoietic cells. Blood 1992;80:3044–3050.
43 O'Reilly MS, Boehm T, Shing Y et al. Endostatin: An endogenous inhibitor of angiogenesis and tumor growth. Cell 1997;88:277–285.
44 Kimble DP. Hippocampus and internal inhibition. Psychol Bull 1968; 70:285–295.
45 Beck H, Voswinckel R, Wagner S et al. Participation of bone marrow-derived cells in long-term repair processes after experimental stroke. J Cereb Blood Flow Metab 2003;23:709–717.
46 Li TS, Furutani A, Takahashi M et al. Impaired potency of bone marrow mononuclear cells for inducing therapeutic angiogenesis in obese diabetic rats. Am J Physiol Heart Circ Physiol 2006;290:H1362–H1369.
47 Ribeiro-Resende VT, Pimentel-Coelho PM, Mesentier-Louro LA et al. Trophic activity derived from bone marrow mononuclear cells increases peripheral nerve regeneration by acting on both neuronal and glial cell populations. Neuroscience 2009;159:540–549.
48 Labouyrie E, Dubus P, Groppi A et al. Expression of neurotrophins and their receptors in human bone marrow. Am J Pathol 1999;154: 405–415.
49 Mahmood A, Lu D, Chopp M. Intravenous administration of marrow stromal cells (MSCs) increases the expression of growth factors in rat brain after traumatic brain injury. J Neurotrauma 2004;21:33–39.
50 Kurozumi K, Nakamura K, Tamiya T et al. Mesenchymal stem cells that produce neurotrophic factors reduce ischemic damage in the rat middle cerebral artery occlusion model. Mol Ther 2005;11:96–104.
51 Hamano K, Li TS, Kobayashi T et al. Angiogenesis induced by the implantation of self-bone marrow cells: A new material for therapeutic angiogenesis. Cell Transplant 2000;9:439–443.
52 Chen J, Li Y, Katakowski M et al. Intravenous bone marrow stromal cell therapy reduces apoptosis and promotes endogenous cell proliferation after stroke in female rat. J Neurosci Res 2003;73:778–786.
53 Connolly DT. Vascular permeability factor: A unique regulator of blood vessel function. J Cell Biochem 1991;47:219–223.
54 Schott RJ, Morrow LA. Growth factors and angiogenesis. Cardiovasc Res 1993;27:1155–1161.
55 Zhu W, Fan Y, Hao Q et al. Postischemic IGF-1 gene transfer promotes neurovascular regeneration after experimental stroke. J Cereb Blood Flow Metab 2009;29:1528–1537.
56 Zhao X, Lu X, Feng Q. Deficiency in endothelial nitric oxide synthase impairs myocardial angiogenesis. Am J Physiol Heart Circ Physiol 2002;283:H2371–H2378.
57 Dore-Duffy P, Katychev A, Wang X et al. CNS microvascular pericytes exhibit multipotential stem cell activity. J Cereb Blood Flow Metab 2006;26:613–624.
58 Shen Q, Wang Y, Kokovay E et al. Adult SVZ stem cells lie in a vascular niche: A quantitative analysis of niche cell-cell interactions. Cell Stem Cell 2008;3:289–300.
59 Capela A, Temple S. LeX/ssea-1 is expressed by adult mouse CNS stem cells, identifying them as nonependymal. Neuron 2002;35:865–875.
60 Stubbs D, Deproto J, Nie K et al. Neurovascular congruence during cerebral cortical development. Cereb Cortex 2009;19:i32–i41.
61 Javaherian A, Kriegstein A. A stem cell niche for intermediate progenitor cells of the embryonic cortex. Cereb Cortex 2009;19:i70–i77.
62 Onda T, Honmou O, Harada K et al. Therapeutic benefits by human mesenchymal stem cells (hMSCs) and Ang-1 gene-modified hMSCs after cerebral ischemia. J Cereb Blood Flow Metab 2008;28:329–340.
63 Gertz K, Priller J, Kronenberg G et al. Physical activity improves long-term stroke outcome via endothelial nitric oxide synthase-dependent augmentation of neovascularization and cerebral blood flow. Circ Res 2006;99:1132–1140.
64 Mori S, Sadoshima S, Ibayashi S et al. Relation of cerebral blood flow to motor and cognitive functions in chronic stroke patients. Stroke 1994;25:309–317.
65 Demchuk AM, Burgin WS, Christou I et al. Thrombolysis in brain ischemia (TIBI) transcranial Doppler flow grades predict clinical severity, early recovery, and mortality in patients treated with intravenous tissue plasminogen activator. Stroke 2001;32:89–93.

See www.StemCells.com for supporting information available online.

BRAIN RESEARCH 1340 (2010) 70–80

available at www.sciencedirect.com

ScienceDirect

www.elsevier.com/locate/brainres

BRAIN RESEARCH

Research Report

Telmisartan suppresses cerebral injury in a murine model of transient focal ischemia

Yukiko Kasahara[a], *Akihiko Taguchi*[a,*], *Hisakazu Uno*[a], *Akiko Nakano*[b], *Takayuki Nakagomi*[b], *Haruka Hirose*[a], *David M. Stern*[c], *Tomohiro Matsuyama*[b]

[a]*Department of Cerebrovascular Disease, National Cardiovascular Center, Osaka, Japan*
[b]*Institute for Advanced Medical Sciences, Hyogo College of Medicine, Hyogo, Japan*
[c]*VPHA and Dean's Office, College of Medicine, University of Cincinnati, OH, USA*

ARTICLE INFO

Article history:
Accepted 31 March 2010
Available online 10 April 2010

Keywords:
Angiotensin II type1 receptor blocker
Ischemia/reperfusion cerebral injury
Neuroprotection
PPARγ agonist activity
Anti-inflammation

ABSTRACT

The beneficial effects of angiotensin II type 1 (AT1) receptor blockers (ARB) in cerebrovascular disease have been shown in clinical trials. However, the effects of ARBs vary based on their unique pharmacologic properties. In this study, we focused on telmisartan, a fat-soluble ARB with selective peroxisome proliferator-activated receptor-γ (PPARγ) agonist activity, and investigated its effects on ischemic injury in cerebral vasculature using murine models of both transient and permanent focal ischemia. Analysis by triphenyltetrazolium-staining revealed that pre-treatment of mice with telmisartan reduced stroke volume 72 h after the transient ischemic insult in a dose-dependent manner, though such treatment did not reduce stroke volume due to permanent ischemia. Transient ischemia induced pro-inflammatory adhesion molecules, such as ICAM-1 and P-selectin in the ischemic region, and treatment with telmisartan diminished the expression of these adhesion molecules with diminished infiltration of inflammatory cells. The beneficial effect of telmisartan was attenuated, in part, by administration of a PPARγ antagonist. Treatment with valsartan (an ARB without PPARγ agonist activity) also decreased ischemic injury after transient ischemia, though to a lesser extent than telmisartan. Our findings indicate that telmisartan has a beneficial effect in a murine model of ischemia/reperfusion injury through blockade of AT1 receptors, and, in addition, due to a positive effect via its specific anti-inflammatory PPARγ agonist activity.

* *Corresponding author.* Department of Cerebrovascular Disease, National Cardiovascular Center, 5-7-1 Fujishiro-dai, Suita, Osaka, Japan, 565-8565. Fax: +81 6 6872 7485.
E-mail address: ataguchi@res.ncvc.go.jp (A. Taguchi).

Abbreviations: AT1, angiotensin II type1; ARB, AT1 receptor blockers; RAS, rennin–angiotensin system; PPARγ, peroxisome proliferator-activated receptor-γ; MCA, middle cerebral artery; CBF, cerebral blood flow; DMSO, dimethyl sulfoxide; ICAM-1, intercellular adhesion molecule-1; eNOS, endothelial nitric oxide synthase; ERK1/2, extracellular signal-regulated kinase 1/2; HUVEC, human umbilical cord vein endothelial cells; TTC, 2,3,5-triphenyltetrazolium; PBS, phosphate-buffered saline; SCID, severe combined immunodeficient

0006-8993/$ – see front matter © 2010 Elsevier B.V. All rights reserved.
doi:10.1016/j.brainres.2010.03.101

1. Introduction

The effect of angiotensin II (Ang II) type 1 (AT1) receptor blockers (ARBs) on preventing/limiting cerebral infarction has been shown in a series of clinical trials, including PROGRESS (PROGRESS Collaborative Group., 2001), SCOPE (Lithell et al., 2004) and ONTARGET (Teo et al., 2004). The beneficial effects of ARBs on cardiovascular (including cerebrovascular) disease probably represent a plethora of underlying mechanisms, including anti-inflammatory properties at the level of the vasculature (Wu et al., 2001), increased cerebrovascular compliance and restoration of the eNOS/iNOS ratio (Saavedra et al., 2006), in addition to their effect on blood pressure through blockade of the renin–angiotensin system (RAS).

In experimental transient focal cerebral ischemia, administration of ARBs has been demonstrated to reduce stroke volume and improve neurologic function through their effect on the RAS (Forder et al., 2005; Hamai et al., 2006; Iwai et al., 2004; Kozak et al., 2008; Suzuki and Kanno, 2005). However, the effects of each individual ARB on cerebrovascular disease vary, in part due to the specific pharmacologic features of each agent, such as fat-solubility, potency, stability and other selective properties. In this study, we have focused on telmisartan (Benson et al., 2004), a fat-soluble ARB with selective peroxisome proliferator–activated receptor-γ (PPARγ) agonist activity. We investigated its effects on cerebral ischemia/reperfusion injury using murine models of transient and permanent focal ischemia. In this system, we have evaluated the contribution of PPARγ agonist activity, as well as blockade of the RAS, on ischemia/reperfusion injury.

2. Results

2.1. *Telmisartan reduces infarct volume after ischemia/reperfusion*

In a previous report, we developed a reproducible murine model of stroke by ligation and disconnection of the distal portion of left middle cerebral artery in SCID mice (Taguchi et al., 2004). In this study, we have modified the latter technique to develop a reproducible model of transient ischemia. Occlusion of the left MCA was induced with a nylon thread for 20 min, followed by reperfusion. Similar to permanent MCA occlusion, cerebral infarction was observed in all mice subjected to this method of transient cerebral ischemia after 72 h of reperfusion in the control group (i.e., no telmisartan; untreated control group) (Fig. 1A). To evaluate the effect of telmisartan on cerebral ischemia/reperfusion, mice were fed a range of doses of

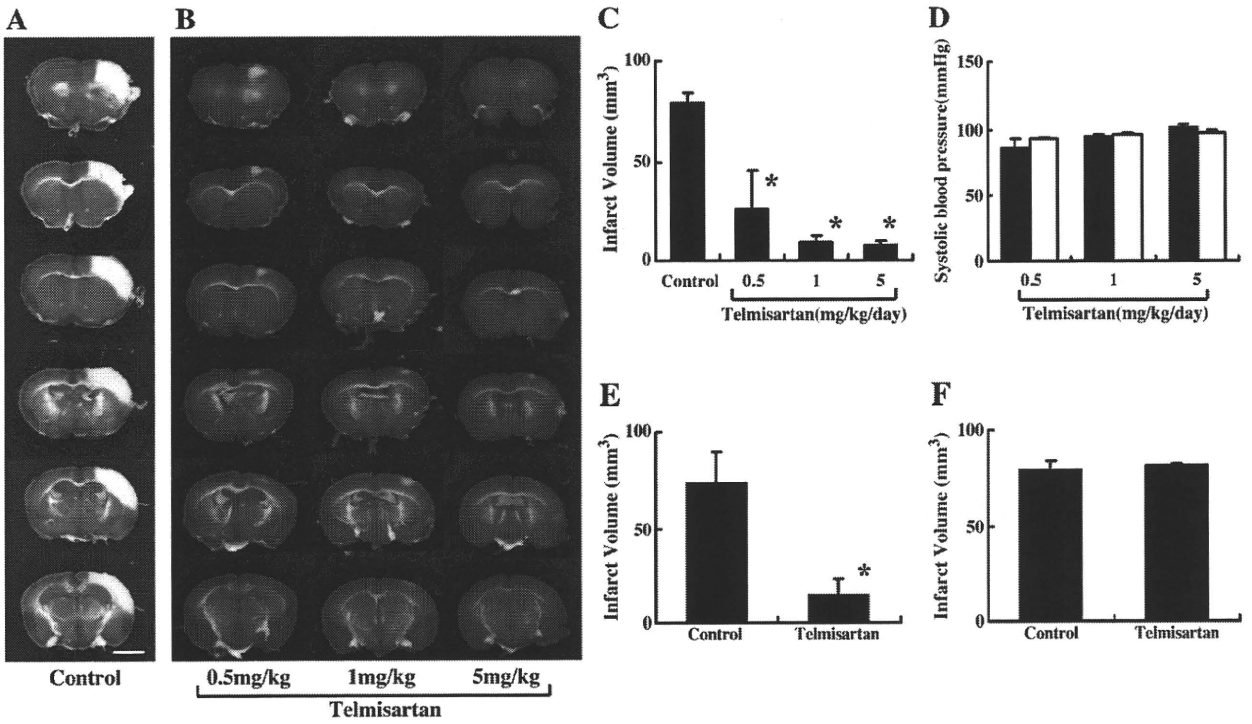

Fig. 1 – Treatment with telmisartan reduced infarct volume after cerebral ischemia/reperfusion. (A–C) Forebrain sections harvested from mice 72 h after stroke were stained with TTC, and lack of positive staining was observed in the whole MCA cortex of control mice (i.e., untreated with telmisartan) (A). In contrast, stroke area was strongly reduced in mice treated with telmisartan (B). Quantitative analysis revealed dose-dependent reduction in stroke volume in mice treated with telmisartan (C). (D) No significant change in blood pressure was observed consequent to treatment with telmisartan (closed bar, before treatment; open bar, after treatment). (E) Treatment with telmisartan in C57BL/6 N mice also resulted in significant suppression of cerebral ischemic injury, compared with controls. (F) In contrast, treatment with telmisartan did not demonstrate a beneficial effect in SCID mice after permanent cerebral occlusion. $n=6$ per group. *$P<0.05$ vs. control. Scale bar, 5 mm.

telmisartan (0.5, 1 or 5 mg/kg/day) for 7 days and transient ischemia was induced. In the presence of telmisartan, ischemia/reperfusion injury was significantly suppressed (Fig. 1B). To quantify the protective effect of telmisartan, the TTC-negative area was calculated, and found to vary in a dose-dependent manner (Fig. 1C). Systolic blood pressure in the tail artery was also measured before and after treatment with telmisartan. Mild, but insignificant, reduction of blood pressure was observed at a dose of 5 mg/kg/day telmisartan (Fig. 1D). The latter observation is consistent with findings in the literature, as the onset of anti-hypertensive effect with ARBs is known to occur over time (Julius et al., 2004). Similarly, previous reports have shown only mild effects of ARBs on blood pressure in normotensive mice after 1 week of treatment (Iwai et al., 2008), though longer treatment periods do significantly reduce blood pressure (Takaya et al., 2006). To exclude the possible influence of the absence of lymphocytes in SCID mice on our results, we also induced cerebral ischemia in immunocompetent C57BL/6 N mice. Though the standard error of infarct volume is considerably larger than that observed in SCID mice, treatment with telmisartan (5 mg/kg) significantly reduced stroke volume (Fig. 1E).

To further investigate the effect of telmisartan on permanent cerebral infarction, SCID mice were treated with telmisartan and permanent occlusion of cerebral artery was induced. At 72 h after induction of ischemia, stroke area was evaluated with TTC staining. In contrast to the beneficial effect observed in our model of transient ischemia, there was no significant reduction of stroke volume with telmisartan observed in the permanent occlusion model, compared with controls (Fig. 1F). Stroke volumes of untreated mice were 81±1 and 80±5 mm^3, in permanent and transient ischemia, respectively ($P=0.25$).

2.2. *Effect of a PPARγ antagonist on ischemia/reperfusion injury*

Telmisartan is known to have selective PPARγ agonist activity, and PPARγ agonists have been shown to exert neuroprotective effects in models of transient cerebral ischemia (Luo et al., 2006; Tureyen et al., 2007). To investigate the potential impact of telmisartan's PPARγ agonist activity in cerebral ischemia/reperfusion, a selective PPARγ antagonist (GW9662; 4 mg/kg) was administered before induction of stroke. In the presence of GW9662, the neuroprotective effect of telmisartan (5 mg/kg) was reduced (Fig. 2A, telmisartan+PBS control; B, telmisartan+GW9662). To confirm the beneficial effect of PPARγ agonist activity, mice were treated with valsartan (10 mg/kg/day), an ARB that lacks PPARγ agonist activity. At 72 h after ischemia, cerebral injury was observed in the MCA area (Fig. 2C). Quantitative analysis revealed that stroke volume was

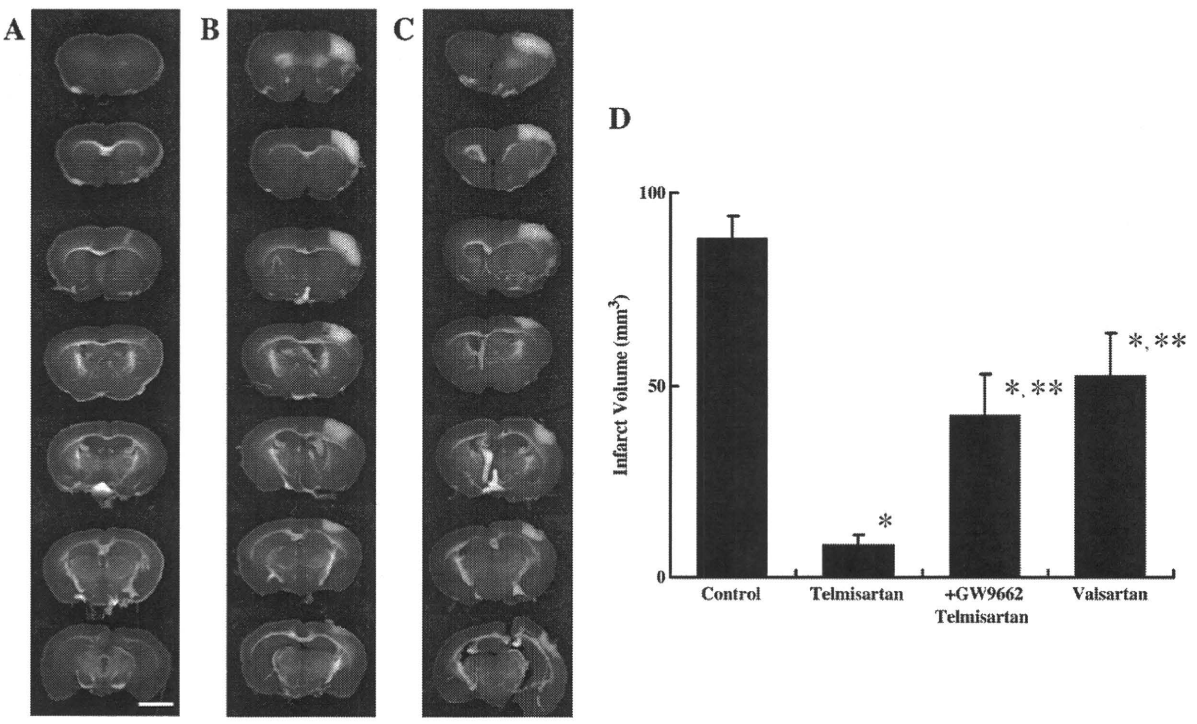

Fig. 2 – Suppression of PPAR-γ activity reduces the beneficial effect of telmisartan in focal cerebral ischemia. (A–C) Representative TTC-stained coronal sections from mice subject to transient focal cerebral ischemia and treated with telmisartan + PBS (A), telmisartan + PPARγ antagonist (GW9662)(B) or valsartan (C). Animals were sacrificed 72 h after ischemic injury. Quantitative analysis confirmed that administration of GW9662 diminished the beneficial effect of telmisartan (C). Similarly, valsartan treatment resulted in a neuroprotective effect, though not to the same extent as telmisartan. It is notable that treatment of mice with telmisartan + GW9662 and valsartan showed a mild, though still significant, neuroprotective effect, compared with untreated mice (F). $n=6$ per group in each experiment. *$P<0.05$ vs. control. **$P<0.05$ vs. telmisartan (C). Scale bar, 5 mm.

significantly increased in animals treated with the telmisartan+ PPARγ antagonist, compared with treatment with telmisartan alone (Fig. 2D). Similarly, stroke volume in valsartan-treated mice was significantly greater, compared with mice receiving telmisartan, though there was a significant reduction in stroke volume in all treated groups (telmisartan, telmisartan+GW9662 and valsartan), compared with non-treated animal. It is notable that there was no significant difference in stroke size between telmisartan+GW9662 and valsartan-treated mice. These results suggest that the beneficial effect of telmisartan on stroke volume was due to both its properties as an ARB and an agonist of PPARγ. Similar to the data with telmisartan, no significant change in blood pressure was observed consequent to treatment of mice with valsartan (96±2 and 100±2 mm Hg, before and after treatment, respectively).

To further confirm the role of telmisartan's PPARγ activity in neuroprotection, mice were treated with the PPARγ-antagonist (GW9662) or valsartan + GW9662. Compared with PBS controls, administration of GW9662 did not significantly affect stroke volume (79±5 and 81±3 mm^3, PBS and GW9662-treatment groups, respectively. $P=0.72$). Similarly, administration of GW9662 to mice treated with valsartan did not affect stroke volume (47±10 and 49±7 mm^3, PBS and GW9662-treatment, respectively. $P=0.87$).

2.3. *Telmisartan improves neurologic function after focal cerebral ischemia*

To investigate neurologic function after focal cerebral ischemia, cortical function was evaluated using the elevated plus-maze test 72 h after MCA occlusion ($n=6$, for each group). ANOVA analysis revealed significant improvement of cortical function in mice treated with telmisartan (5 mg/kg), compared with untreated controls (Fig. 3A and B). No significant difference in neurologic deficits of motor function was observed comparing animals in all groups, based on evaluation using the 3-pointed test (0.00±0.0, 0.50±0.2, 0.17±0.2, 0.33±0.2, and 0.33±0.2, in sham, control, telmisartan, GW + telmisartan and valsartan groups, respectively. $P=0.37$). Body weights were also comparable between the different groups of mice (23.5±0.6, 21.2±0.5, 22.5±0.6, 21.5±0.8 and 22.3±0.4 g, in sham, control, telmisartan, GW + telmisartan and valsartan groups, respectively. $P=0.34$).

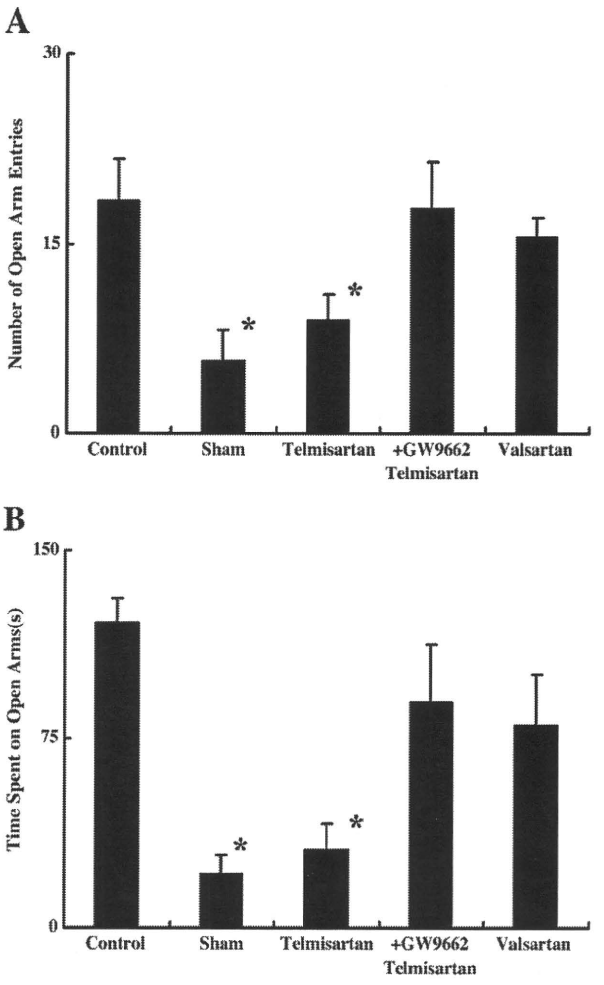

Fig. 3 – Treatment with telmisartan improved behavioral function following transient focal cerebral ischemia. Behavioral function in telmisartan-, valsartan-, telmisartan + GW9662-treated and untreated mice 72 h after transient MCA occlusion in the elevated plus-maze test was studied. Compared with control mice, treatment with telmisartan significantly improved neurological function, with respect to number of open arm entries (A) and time spent in the open arms (B). $n=6$ per group in each experiment. *$P<0.05$ vs. control.

2.4. *Telmisartan suppresses ischemia/reperfusion injury after transient cerebral ischemia*

Reperfusion injury has been shown to up-regulate expression of cell adhesion molecules on endothelium, followed by accumulation of inflammatory cells (Iadecola and Alexander, 2001; Mabuchi et al., 2000). Expression of P-selectin, a cell adhesion molecule that mediates rolling of neutrophils, was observed in the ischemic area at 24, 48 and 72 h after reperfusion in untreated (i.e., control) post-ischemic mice (Fig. 4A–D). Similarly, expression of ICAM-1, a cell adhesion molecule that mediates firm adherence of inflammatory cells, was observed 24, 48 and 72 h after reperfusion (Fig. 4E–H). Co-staining of sections from stroke-affected cortex with antibody to eNOS confirmed that expression of ICAM-1 occurred in endothelial cells (Fig. 4I and J). Treatment with telmisartan (5 mg/kg) significantly attenuated ischemia-induced expression of these pro-inflammatory adhesion molecules at 48 and 72 h after reperfusion (Fig. 4K and L, P-selectin; Fig. 4 M, N, ICAM-1). To evaluate the ongoing inflammatory response triggered by ischemia, we assessed infiltration and activation of inflammatory cells in the ischemic brain using CD11b as a marker. In contrast to the contralateral cortex (Fig. 4O), massive infiltration of CD11b-positive cells was observed in control (i.e., untreated) mice 72 h after reperfusion (Fig. 4P). In contrast, reduced numbers of CD11b-positive cells were observed in mice treated with telmisartan (Fig. 4Q). Compared with untreated mice (Fig. 4R, contralateral; 4S, ipsilateral cortex), suppressed activation of macrophages/microglia, based on staining with F4/80, was observed in telmisartan-treated mice (Fig. 4T). To better quantify these observations, expression of ICAM-1 was evaluated by Western blotting. At 48 h

A
B
C
D
E
F
G
H
I
J
K
L
M
N
O
P
Q
R
S
T
U
sham
control
telmisartan
100kDa
ICAM-1(95kDa)
V
Caspase-3 Activity
(x10-4uMPNA/min/mg tissue)
1
0.5
0
T
*
Control
Telmisartan

after induction of ischemia, expression of ICAM was observed, and this was suppressed by treatment of telmisartan (Fig. 4U). Similarly, the caspase-3 activity in the ischemic cortex was reduced by treatment with telmisartan (Fig. 4V).

2.5. *Telmisartan activates phosphorylation of eNOS and ERK1/2 in vitro*

To investigate the molecular mechanism of the beneficial effect of telmisartan on reperfusion injury, activation of eNOS and MAP kinase was evaluated *in vitro* using human umbilical cord vein endothelial cells (HUVEC). Activation of eNOS is well-known to induce vasodilation immediately after the onset of stroke through production of NO (Han et al., 2006; Li et al., 2009). MAP kinases are serine/threonine-specific protein kinases that regulate critical cellular activities, such as mitosis, differentiation and cell survival/apoptosis (Kant et al., 2006). HUVECs were treated with telmisartan for 2 h and phosphorylation of eNOS, ERK1/2, p38 and JNK1/2 was investigated. Treatment with telmisartan significantly increased phosphorylation of eNOS, compared with PBS controls (Fig. 5A). Telmisartan also increased the phosphorylation of ERK1/2 (Fig. 5B), though no significant change was observed in the level of phosphorylated p38 (Fig. 5C) and JNK1/2 (Fig. 5D).

3. Discussion

Our results demonstrate that pretreatment of mice with telmisartan suppresses brain injury following ischemia/reperfusion and improves stroke outcome, at least in part, through activation PPARγ and blockade of the RAS in a transient focal cerebral ischemia model applied to mice with normal lipoprotein metabolism.

In order to evaluate stroke experimentally, a necessary prerequisite is establishment of a reproducible model of cerebral ischemia/infarction. Previously, we developed such a stroke model using permanent occlusion in SCID mice. This model is suitable for quantification of the effect of cell therapy on neurogenesis, neovessel formation, and neural function (Taguchi et al., 2004). In the current study, we have modified our previous permanent ischemia model to a transient focal cerebral infarction model, and found the latter to also provide highly reproducible data. Using this model, we have demonstrated a beneficial effect of telmisartan in mice subjected to transient cerebral ischemia. The results of the current study are consistent with previous data in immunocompetent apolipoprotein E-deficient mice (Iwai et al., 2008). The beneficial effects of ARBs in ischemia are likely to reflect a range of mechanisms in addition to blockade of the RAS (Forder et al., 2005; Hamai et al., 2006; Iwai et al., 2004; Kozak et al., 2008; Suzuki and Kanno, 2005). Thus, previous reports have shown that administration of ARBs, including telmisartan and valsartan, significantly suppressed ischemic brain injury without inducing a significant change in blood pressure. The latter observations reflect the results of clinical trials in which the advantages of ARBs appear to extend beyond their effects on blood pressure (Berl et al., 2005; Julius et al., 2004; Mochizuki et al., 2007).

The effects of a particular ARB depend not only on inhibition of the RAS, but also on individual pharmacologic properties of the molecule being evaluated. In this study, we have compared telmisartan and valsartan. We have found a milder protective effect of valsartan on cerebral injury following transient ischemia than with telmisartan. This led us to analyze the known PPARγ agonist activity of telmisartan (PPARγ is a transcription factor that regulates expression of a range of inflammatory genes) (Luo et al., 2006; Sundararajan et al., 2005). Recent studies indicate that PPARγ agonists attenuate ischemia-induced activation of microglia, expression of ICAM-1 and neutrophil infiltration in C57BL/6 mice (Luo et al., 2006; Tureyen et al., 2007). Consistent with these results, the beneficial effects of telmisartan were reduced with concomitant administration of GW9662, a PPARγ antagonist. It is notable that co-administration of GW9662 and telmisartan reduced the neuroprotective benefit of telmisartan to the level observed with valsartan, an ARB devoid of PPARγ agonist activity.

Expression of ICAM-1 is induced by ischemia/reperfusion, and contributes to accumulation/activation of microglia at the site of injury (del Zoppo et al., 1991). We have found that treatment with telmisartan markedly reduced expression of ICAM-1 in endothelial cells, and suppressed activation of microglia in ischemic brain. These findings indicate that a potential benefit of telmisartan on ischemic brain may be achieved, at least in part, through modulation of the

Fig. 4 – Treatment with telmisartan suppressed ischemia-induced inflammation in the transient stroke model. (A–D) Expression of P-selectin was observed at 24 (A), 48 (B) and 72 h (C) after ischemia in untreated mice (C, lower magnification; D, higher magnification). (E–J) Similarly, expression of ICAM-1 was observed at 24 (E), 48 (F) and 72 h (G, lower magnification; H, higher magnification) after induction of ischemia in the post-ischemic cortex. It is notable that the expression of ICAM-1 at ischemic core was considerably decreased at 72 h (G), compared with 48 h (F) after ischemia. Expression of ICAM-1 in endothelial cells was confirmed by co-staining with eNOS (I, eNOS; J, eNOS [green] and ICAM-1 [red]). (K–N) In contrast, brains from telmisartan-treated mice subjected to transient cerebral ischemia showed significantly reduced expression of P-Selectin (K, 48 h; L, 72 h) and ICAM-1 (M, 48 h; N, 72 h) after reperfusion. (O–T) Infiltration of CD11b-positive cells into the ischemic area was observed in untreated mice at 72 h after reperfusion (O, contralateral; P, ipsilateral). In contrast, reduced numbers of CD11b-positive cells were observed in telmisartan-treated mice (Q). Similarly, activation of F4/80$^+$ macrophages/microglia was observed in the post-ischemic area in untreated mice (R, contralateral; S, ipsilateral), though reduced numbers of F4/80$^+$ cells were observed in telmisartan-treated mice (T) at 72 h after reperfusion. (U), Analysis of protein extracts from the ischemic area at 48 h after ischemia confirmed suppressed expression of ICAM-1, consequent to treatment with telmisartan. Representative results are shown in 3 repeated experiments. (V) The level of caspase-3 activity in the ischemic region was significantly increased in control mice compared with telmisartan treated mice ($n=3$). Scale bars, 150 μm (A, O), 35 μm (D, H) and 400 μm (E, K). *$P<0.05$ vs. control.

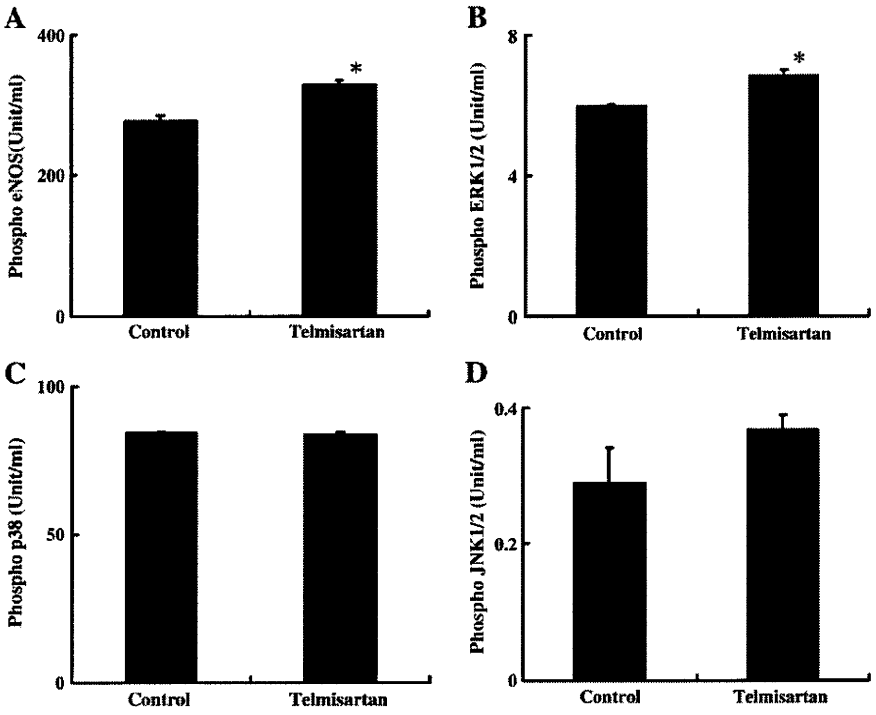

Fig. 5 – Telmisartan administration results in activation of eNOS and ERK1/2 in endothelial cells *in vitro*. (A) eNOS of endothelial cells was activated in the presence of telmisartan. (B) In contrast to the activation of ERK1/2 (B) observed in the presence of telmisartan, there was no change in the level of phosphorylated p38 (C) or JNK1/2 (D). *P<0.05 vs. PBS control.

inflammatory properties of endothelium, in addition to direct neuroprotection. Consistent with this concept, telmisartan-treated mice displayed reduced expression of P-selectin, an essential contributor to the aggregation of platelets and the initial recruitment of leukocytes at the endothelial interface (Woollard, 2005) in ischemic cerebral cortex.

In this article, we have shown that administration of telmisartan suppressed ischemic brain damage after transient ischemia, but not permanent occlusion of the MCA. *In vitro* analysis revealed that telmisartan increased phosphorylation of eNOS and ERK1/2 in endothelial cells. Activation of ERK1/2 has been shown to suppress apoptotic cell death after reperfusion injury. Activation of eNOS is also known to suppress inflammatory damage by inhibiting expression of vascular cell adhesion molecule and leukocyte tissue infiltration following ischemia-reperfusion (Kaminski et al., 2004; Li et al., 2009). Although production of NO in the presence of peroxides could enhance endothelial dysfunction through formation of peroxynitrite, resulting in oxidation and nitration of proteins, telmisartan has been shown to suppress oxidation and nitration by suppressing up-regulation of NADPH via PPARγ agonist activity (Kagota et al., 2007; Wenzel et al., 2008). These findings potentially explain our results that administration of telmisartan suppressed expression of cell adhesion molecules and significantly reduced brain damage after transient ischemia, compared with valsartan.

In contrast, permanent occlusion of MCA serves more severe ischemia that induces necrotic neuronal cell death directly, though the production of superoxide and formation of nitrotyrosine are much less, compared with transient ischemia (Takizawa et al., 2003). Furthermore, depletion of tetrahydrobioptein (BH4: an essential cofactor for eNOS enzymatic activity) under permanent ischemic condition causes eNOS dysfunction that results in increased production of superoxide, rather than NO (Sasaki et al., 2008). These findings may explain the reason why administration of telmisartan has little effect on preventing ischemic brain damage after permanent ligation of MCA.

Although our model in SCID mice has limitations, especially since the influence of lymphocytes cannot be evaluated, this highly reproducible transient cerebral ischemia model enables us to more accurately quantify of stroke volume. Combined with previous findings in immunocompetent mice, our results indicate that telmisartan suppresses ischemic brain injury in a murine transient focal cerebral infarction model through blockade of AT1 receptors and PPARγ agonist activity. Reduction of stroke volume might be associated with anti-inflammatory activities related to PPARγ agonist activity of telmisartan in the ischemic region. These observations may point to an added beneficial effect of telmisartan in a range of ischemic settings where other ARBs would not be as efficacious. Recently, results from a multicenter, double-blind, randomized, placebo-controlled trial of telmisartan for prevention of recurrent stroke in the patients who had an ischemic stroke were reported (Yusuf et al., 2008) (the median follow-up was 2.5 years). Although there was no significant difference in the number of patients with recurrent stroke in the telmisartan group compared to the placebo group (8.7% vs. 9.2%, respectively; hazard ratio [HR] 0.95, 95% confidence interval [CI] 0.86-1.04), post hoc exploratory analyses indicated that the rate of recurrent stroke beyond 6 months of the trial was lower in the telmisartan group (5.3% vs. 6.0%, respectively; HR 0.88, 95% CI

0.78-0.99). Combined with our results showing that telmisartan has vasculoprotective effects, these clinical observations suggest that long-term treatment of telmisartan might be beneficial for preventing stroke. Further clinical trials will be needed to elucidate the beneficial effect of telmisartan, achieved through blockade of AT1 receptors and its PPARγ agonist activity, for preventing ischemic cerebrovascular diseases in humans.

4. Experimental procedures

All procedures were performed under auspices of an approved protocol of the National Cardiovascular Center Animal Care and Use Committees.

4.1. *Induction of focal cerebral ischemia*

To assess the effect of telmisartan after ischemia/reperfusion injury, we developed a highly reproducible murine transient cerebral ischemia model based on a modification of our previous method (Taguchi et al., 2004). In brief, transient focal cerebral ischemia was induced in male 7 week SCID mice (Oriental Yeast Co. Ltd., Tokyo, Japan) under halothane inhalation (3%) anesthesia by occluding the distal portion of the left middle cerebral artery (MCA) with a monofilament nylon suture (7-0 in size, Tyco, USA) for 20 min. During surgery, rectal temperature was monitored and controlled at 37.0±0.2 °C by a feedback-regulated heating pad. Cerebral blood flow (CBF) in the MCA area was monitored as described (Matsushita et al., 1998). All mice subjected to the above operative procedure showed ~75% decreased CBF in the MCA as soon as the occlusion period commenced, and ~80% restoration of CBF immediately after the occlusion was relieved, based on comparison with CBF before occlusion (the success rate of the procedure with these outcomes was >90%). The size of the infarct produced in this transient cerebral ischemia model, with an ischemic period of 20 min, was comparable to that observed with permanent occlusion of the MCA. In sham operated control groups, mice were operated on using the same procedure, except ligation of cerebral artery was omitted. No animal demonstrated more than 15% decrease of CBF during the procedure. In another variation of the protocol, we investigated the effect of telmisartan on permanent cerebra ischemia. Permanent occlusion model was undertaken in SCID mice by ligation and dissociation of left MCA as described previously (Taguchi et al., 2004).

To exclude the possible influence of the absence of the lymphocytes in SCID mice, additional studies were performed in C57BL/6 N animals (Oriental Yeast) using the same methods described above using 30 min of ischemia. The effect of telmisartan was evaluated as above and the result is shown in Fig. 1E. All other *in vivo* experiments were performed using our highly reproducible stroke model in SCID mice.

4.2. *Drug administration*

Mice were fed telmisartan (0.5, 1 or 5 mg/kg/day: Boehringer Ingelheim, Ingelheim, Germany) for 7 days before induction of ischemia. Control mice were fed the same diet without telmisartan. A group of mice treated with valsartan (10 mg/kg/day; Novartis, Basel), an ARB without PPARγ agonist activity, was also employed as controls. The potency of telmisartan has been shown to be about twice that of valsartan in terms of AT1 receptor antagonism (Calvo et al., 2004; Mori et al., 2007). Doses of telmisartan and valsartan were selected according to the previous reports (Araki et al., 2006; Nagai et al., 2006). Systolic blood pressure was measured twice before treatment with the ARBs, and before induction of cerebral ischemia which corresponded to 7 days after initiation of drug treatment. The indirect tail-cuff method with a blood pressure monitor (MK-2000ST; Muromachi Kikai, Japan) was employed. All measurements were repeated five times for each animal. GW9662 (PPARγ antagonist; Sigma-Aldrich, St. Louis, MO, USA) was dissolved in dimethyl sulfoxide (DMSO; Sigma) and diluted in PBS to decrease the DMSO concentration to 3%. GW9662 was injected intraperitoneally (i.p.) 1 h before MCA occlusion.

4.3. *Immunohistochemistry*

Brains were removed and fixed in paraformaldehyde. Coronal sections (20 μm) were prepared using a vibratome (Leica, Wetzlar, Germany) and immunostained with antibodies to intercellular adhesion molecule-1 (ICAM; BD Pharmingen, San Jose, CA, USA; dilution 1:200), endothelial nitric oxide synthase (eNOS; BD Pharmingen; dilution 1:500), P-selectin (Santa Cruz Biotechnology, Santa Cruz, CA, USA; dilution 1:500), CD11b (Serotec, Raleigh, NC, USA; dilution 1:250) and F4/80 (Serotec; dilution 1:50) using standard immunohistochemical procedures. Anti-P-selectin or ICAM antibody was labeled with red fluorescence (donky-anti-goat, Chemicon, Temecula, CA; dilution 1:100, or streptavidin-Cy3, Sigma; dilution; 1:1000), and anti-eNOS antibody was labeled with green fluorescence (goat-anti-mouse, Jackson Immuno Research, West Grove, PA; dilution 1:100). Cells expressing CD11b or F4/80 were visualized by DAB reaction.

4.4. *Estimation of infarct volume*

Infarct volume was evaluated 72 h after induction of ischemia as described previously (Hata et al., 1998; Saavedra et al., 2006). Briefly, the forebrain of samples harvested 72 h after MCA occlusion was sectioned coronally (1 mm sections), and the latter were stained with 1% 2,3,5-triphenyltetrazolium (TTC: Sigma-Aldrich, St. Louis, MO, USA) for 20 min at 37 °C, and then fixed in 4% paraformaldehyde/phosphate-buffered saline (PBS; pH 7.4). Infarct volume was measured using a microscopic digital camera system (Olympus, Tokyo, Japan). The volume of viable cortex was estimated using NIH Image software.

4.5. *Behavioral tests*

To assess cortical function, mice were subjected to behavioral testing using the elevated plus-maze test 72 h after MCA occlusion as described (Nakashima et al., 2003). Briefly, the plus-maze was made of plexiglass and consisted of two opposite open arms (24×8 cm) and two enclosed arms with side and end walls. The height of each arm was 50 cm from the floor. At the beginning of the test, each mouse was placed at the center of the plus-maze facing one of the open arms, and the cumulative time

spent on the open arms and the number of open arm entries was measured during a 30-min observation period. To exclude the contribution of physical deficits directly related to the operative procedure and induction of stroke, motor deficiencies were examined at the same time point after MCA occlusion. Neurologic deficits were scored on a 3-point modified scale: no neurological deficit (0); failure to extend the left forepaw fully (1); circling to left (2); loss of walking or righting reflex (3), as described (Tamatani et al., 2001).

4.6. *Western blotting*

At 48 h after induction of ischemia, protein extracts were obtained from the ischemic cortical area, and expression of ICAM-1 was evaluated by Western blotting as described previously (Taguchi et al., 2000). Briefly, protein was extracted using a total protein extraction kit (Bio-RAD, Hercules, CA, USA) and immunoblotting was performed on the protein extract (20 μg) using anti-ICAM (BD Pharmingen) antibody.

4.7. *Quantification of caspase-3 activity*

The activity of caspase-3 was examined using a caspase-3 assay kit (Sigma-Aldrich) according to manufacturer's protocol. Briefly, at 48 h after induction of ischemia, tissues from the ischemic area were homogenized in lysis buffer and centrifuged at 20,000×g for 15 min. Supernatants were mixed with assay buffer and caspase-3 substrate. Absorbance at 405 nm was measured and caspase-3 activity was calculated (n=3 in each group).

4.8. *In vitro analysis of endothelial nitric oxide synthase (eNOS) and MAP kinases*

To investigate the effects of telmisartan on vascular endothelium, activation of eNOS, extracellular signal-regulated kinase 1/2 (ERK1/2), p38 and JNK1/2 was investigated *in vitro* using human umbilical vein endothelial cells (HUVEC; Kurabo, Osaka, Japan). Approximately 80% confluent HUVEC cells were treated with telmisartan (5 μg/ml) for 2 h in HuMedia-medium (Kurabo) without FBS. The level of phosphorylation of each of the above targets was evaluated according to manufacturer's protocol (cytometric bead array kit; BD Biosciences). Briefly, after aspiration of all medium, cells were denatured and lysed with denaturation buffer (Cell Signaling Master Buffer Kit; BD Biosciences) containing protease inhibitors (Sigma Chemical) and phosphatase inhibitors (Sigma Chemical). After boiling for 5 min, protein samples were treated with a high quality DNase 1 (Sigma Chemical) for 15 min. The level of phosphorylation was analyzed using anti-phosphorylated eNOS (Ser-1177), ERK1/2 (Thr-202 and Tyr-204), p38 (Thr-180 and Tyr-182) and JNK1/2 (Thr-183 and Tyr-185) by FACS Canto (BD Bioscience).

4.9. *Data analysis*

Statistical comparisons among groups were determined using one-way analysis of variance (ANOVA) and the Dunnett test was used for post-hoc analysis to compare with controls. Where indicated, individual comparisons were performed using Student's t-test. Data were expressed as mean ± standard error (s.e.).

Acknowledgments

This work was supported by a Grant from Japan Cardiovascular Research Foundation (H19-Choujyu-029).

REFERENCES

Araki, K., Masaki, T., Katsuragi, I., Tanaka, K., Kakuma, T., Yoshimatsu, H., 2006. Telmisartan prevents obesity and increases the expression of uncoupling protein 1 in diet-induced obese mice. Hypertension 48, 51–57.

Benson, S.C., Pershadsingh, H.A., Ho, C.I., Chittiboyina, A., Desai, P., Pravenec, M., Qi, N., Wang, J., Avery, M.A., Kurtz, T.W., 2004. Identification of telmisartan as a unique angiotensin II receptor antagonist with selective PPARgamma-modulating activity. Hypertension 43, 993–1002.

Berl, T., Hunsicker, L.G., Lewis, J.B., Pfeffer, M.A., Porush, J.G., Rouleau, J.L., Drury, P.L., Esmatjes, E., Hricik, D., Pohl, M., Raz, I., Vanhille, P., Wiegmann, T.B., Wolfe, B.M., Locatelli, F., Goldhaber, S.Z., Lewis, E.J., 2005. Impact of achieved blood pressure on cardiovascular outcomes in the Irbesartan Diabetic Nephropathy Trial. J. Am. Soc. Nephrol. 16, 2170–2179.

Calvo, C., Hermida, R.C., Ayala, D.E., Ruilope, L.M., 2004. Effects of telmisartan 80 mg and valsartan 160 mg on ambulatory blood pressure in patients with essential hypertension. J. Hypertens. 22, 837–846.

del Zoppo, G.J., Schmid-Schonbein, G.W., Mori, E., Copeland, B.R., Chang, C.M., 1991. Polymorphonuclear leukocytes occlude capillaries following middle cerebral artery occlusion and reperfusion in baboons. Stroke 22, 1276–1283.

Forder, J.P., Munzenmaier, D.H., Greene, A.S., 2005. Angiogenic protection from focal ischemia with angiotensin II type 1 receptor blockade in the rat. Am. J. Physiol. Heart Circ. Physiol. 288, H1989–H1996.

Hamai, M., Iwai, M., Ide, A., Tomochika, H., Tomono, Y., Mogi, M., Horiuchi, M., 2006. Comparison of inhibitory action of candesartan and enalapril on brain ischemia through inhibition of oxidative stress. Neuropharmacology 51, 822–828.

Han, F., Shirasaki, Y., Fukunaga, K., 2006. Microsphere embolism-induced endothelial nitric oxide synthase expression mediates disruption of the blood–brain barrier in rat brain. J. Neurochem. 99, 97–106.

Hata, R., Mies, G., Wiessner, C., Fritze, K., Hesselbarth, D., Brinker, G., Hossmann, K.A., 1998. A reproducible model of middle cerebral artery occlusion in mice: hemodynamic, biochemical, and magnetic resonance imaging. J. Cereb. Blood Flow Metab. 18, 367–375.

Iadecola, C., Alexander, M., 2001. Cerebral ischemia and inflammation. Curr. Opin. Neurol. 14, 89–94.

Iwai, M., Liu, H.W., Chen, R., Ide, A., Okamoto, S., Hata, R., Sakanaka, M., Shiuchi, T., Horiuchi, M., 2004. Possible inhibition of focal cerebral ischemia by angiotensin II type 2 receptor stimulation. Circulation 110, 843–848.

Iwai, M., Inaba, S., Tomono, Y., Kanno, H., Iwanami, J., Mogi, M., Horiuchi, M., 2008. Attenuation of focal brain ischemia by telmisartan, an angiotensin II type 1 receptor blocker, in atherosclerotic apolipoprotein E-deficient mice. Hypertens. Res. 31, 161–168.

Julius, S., Kjeldsen, S.E., Weber, M., Brunner, H.R., Ekman, S., Hansson, L., Hua, T., Laragh, J., McInnes, G.T., Mitchell, L., Plat,

F., Schork, A., Smith, B., Zanchetti, A., 2004. Outcomes in hypertensive patients at high cardiovascular risk treated with regimens based on valsartan or amlodipine: the VALUE randomised trial. Lancet 363, 2022–2031.

Kagota, S., Tada, Y., Kubota, Y., Nejime, N., Yamaguchi, Y., Nakamura, K., Kunitomo, M., Shinozuka, K., 2007. Peroxynitrite is involved in the dysfunction of vasorelaxation in SHR/NDmcr-cp rats, spontaneously hypertensive obese rats. J. Cardiovasc. Pharmacol. 50, 677–685.

Kaminski, A., Pohl, C.B., Sponholz, C., Ma, N., Stamm, C., Vollmar, B., Steinhoff, G., 2004. Up-regulation of endothelial nitric oxide synthase inhibits pulmonary leukocyte migration following lung ischemia-reperfusion in mice. Am. J. Pathol. 164, 2241–2249.

Kant, S., Schumacher, S., Singh, M.K., Kispert, A., Kotlyarov, A., Gaestel, M., 2006. Characterization of the atypical MAPK ERK4 and its activation of the MAPK-activated protein kinase MK5. J. Biol. Chem. 281, 35511–35519.

Kozak, W., Kozak, A., Johnson, M.H., Elewa, H.F., Fagan, S.C., 2008. Vascular protection with candesartan after experimental acute stroke in hypertensive rats: a dose-response study. J. Pharmacol. Exp. Ther. 326, 773–782.

Li, J., Wu, F., Zhang, H., Fu, F., Ji, L., Dong, L., Li, Q., Liu, W., Zhang, Y., Lv, A., Wang, H., Ren, J., Gao, F., 2009. Insulin inhibits leukocyte-endothelium adherence via an Akt-NO-dependent mechanism in myocardial ischemia/reperfusion. J. Mol. Cell. Cardiol. 47, 512–519.

Lithell, H., Hansson, L., Skoog, I., Elmfeldt, D., Hofman, A., Olofsson, B., Trenkwalder, P., Zanchetti, A., 2004. The Study on COgnition and Prognosis in the Elderly (SCOPE); outcomes in patients not receiving add-on therapy after randomization. J. Hypertens. 22, 1605–1612.

Luo, Y., Yin, W., Signore, A.P., Zhang, F., Hong, Z., Wang, S., Graham, S.H., Chen, J., 2006. Neuroprotection against focal ischemic brain injury by the peroxisome proliferator-activated receptor-gamma agonist rosiglitazone. J. Neurochem. 97, 435–448.

Mabuchi, T., Kitagawa, K., Ohtsuki, T., Kuwabara, K., Yagita, Y., Yanagihara, T., Hori, M., Matsumoto, M., 2000. Contribution of microglia/macrophages to expansion of infarction and response of oligodendrocytes after focal cerebral ischemia in rats. Stroke 31, 1735–1743.

Matsushita, K., Matsuyama, T., Nishimura, H., Takaoka, T., Kuwabara, K., Tsukamoto, Y., Sugita, M., Ogawa, S., 1998. Marked, sustained expression of a novel 150-kDa oxygen-regulated stress protein, in severely ischemic mouse neurons. Brain Res. Mol. Brain Res. 60, 98–106.

Mochizuki, S., Dahlof, B., Shimizu, M., Ikewaki, K., Yoshikawa, M., Taniguchi, I., Ohta, M., Yamada, T., Ogawa, K., Kanae, K., Kawai, M., Seki, S., Okazaki, F., Taniguchi, M., Yoshida, S., Tajima, N., 2007. Valsartan in a Japanese population with hypertension and other cardiovascular disease (Jikei Heart Study): a randomised, open-label, blinded endpoint morbidity-mortality study. Lancet 369, 1431–1439.

Mori, Y., Itoh, Y., Tajima, N., 2007. Angiotensin II receptor blockers downsize adipocytes in spontaneously type 2 diabetic rats with visceral fat obesity. Am. J. Hypertens. 20, 431–436.

Nagai, N., Oike, Y., Izumi-Nagai, K., Urano, T., Kubota, Y., Noda, K., Ozawa, Y., Inoue, M., Tsubota, K., Suda, T., Ishida, S., 2006. Angiotensin II type 1 receptor-mediated inflammation is required for choroidal neovascularization. Arterioscler. Thromb. Vasc. Biol. 26, 2252–2259.

Nakashima, M.N., Ajiki, K., Nakashima, K., Takahashi, M., 2003. Possible role of nitric oxide in anxiety following transient cerebral ischemia in mice. J. Pharmacol. Sci. 91, 47–52.

PROGRESS Collaborative Group, 2001. Randomised trial of a perindopril-based blood-pressure-lowering regimen among 6, 105 individuals with previous stroke or transient ischaemic attack. Lancet 358, 1033–1041.

Saavedra, J.M., Benicky, J., Zhou, J., 2006. Mechanisms of the anti-ischemic effect of angiotensin II AT(1) receptor antagonists in the brain. Cell. Mol. Neurobiol. 26, 1099–1111.

Sasaki, N., Yamashita, T., Takaya, T., Shinohara, M., Shiraki, R., Takeda, M., Emoto, N., Fukatsu, A., Hayashi, T., Ikemoto, K., Nomura, T., Yokoyama, M., Hirata, K., Kawashima, S., 2008. Augmentation of vascular remodeling by uncoupled endothelial nitric oxide synthase in a mouse model of diabetes mellitus. Arterioscler. Thromb. Vasc. Biol. 28, 1068–1076.

Sundararajan, S., Gamboa, J.L., Victor, N.A., Wanderi, E.W., Lust, W.D., Landreth, G.E., 2005. Peroxisome proliferator-activated receptor-gamma ligands reduce inflammation and infarction size in transient focal ischemia. Neuroscience 130, 685–696.

Suzuki, H., Kanno, Y., 2005. Effects of candesartan on cardiovascular outcomes in Japanese hypertensive patients. Hypertens. Res. 28, 307–314.

Taguchi, A., Blood, D.C., del Toro, G., Canet, A., Lee, D.C., Qu, W., Tanji, N., Lu, Y., Lalla, E., Fu, C., Hofmann, M.A., Kislinger, T., Ingram, M., Lu, A., Tanaka, H., Hori, O., Ogawa, S., Stern, D.M., Schmidt, A.M., 2000. Blockade of RAGE-amphoterin signalling suppresses tumour growth and metastases. Nature 405, 354–360.

Taguchi, A., Soma, T., Tanaka, H., Kanda, T., Nishimura, H., Yoshikawa, H., Tsukamoto, Y., Iso, H., Fujimori, Y., Stern, D.M., Naritomi, H., Matsuyama, T., 2004. Administration of CD34+ cells after stroke enhances neurogenesis via angiogenesis in a mouse model. J. Clin. Invest. 114, 330–338.

Takaya, T., Kawashima, S., Shinohara, M., Yamashita, T., Toh, R., Sasaki, N., Inoue, N., Hirata, K., Yokoyama, M., 2006. Angiotensin II type 1 receptor blocker telmisartan suppresses superoxide production and reduces atherosclerotic lesion formation in apolipoprotein E-deficient mice. Atherosclerosis 186, 402–410.

Takizawa, S., Fukuyama, N., Hirabayashi, H., Nakazawa, H., Shinohara, Y., 2003. Reperfusion enhances nitrotyrosine formation in rat focal cerebral ischemia. J. Stroke Cerebrovasc. Dis. 12, 196–200.

Tamatani, M., Matsuyama, T., Yamaguchi, A., Mitsuda, N., Tsukamoto, Y., Taniguchi, M., Che, Y.H., Ozawa, K., Hori, O., Nishimura, H., Yamashita, A., Okabe, M., Yanagi, H., Stern, D.M., Ogawa, S., Tohyama, M., 2001. ORP150 protects against hypoxia/ischemia-induced neuronal death. Nat. Med. 7, 317–323.

Teo, K., Yusuf, S., Sleight, P., Anderson, C., Mookadam, F., Ramos, B., Hilbrich, L., Pogue, J., Schumacher, H., 2004. Rationale, design, and baseline characteristics of 2 large, simple, randomized trials evaluating telmisartan, ramipril, and their combination in high-risk patients: the Ongoing Telmisartan Alone and in Combination with Ramipril Global Endpoint Trial/Telmisartan Randomized Assessment Study in ACE Intolerant Subjects with Cardiovascular Disease (ONTARGET/TRANSCEND) trials. Am. Heart J. 148, 52–61.

Tureyen, K., Kapadia, R., Bowen, K.K., Satriotomo, I., Liang, J., Feinstein, D.L., Vemuganti, R., 2007. Peroxisome proliferator-activated receptor-gamma agonists induce neuroprotection following transient focal ischemia in normotensive, normoglycemic as well as hypertensive and type-2 diabetic rodents. J. Neurochem. 101, 41–56.

Wenzel, P., Schulz, E., Oelze, M., Muller, J., Schuhmacher, S., Alhamdani, M.S., Debrezion, J., Hortmann, M., Reifenberg, K., Fleming, I., Munzel, T., Daiber, A., 2008. AT1-receptor blockade by telmisartan upregulates GTP-cyclohydrolase I and protects eNOS in diabetic rats. Free Radic. Biol. Med. 45, 619–626.

Woollard, K.J., 2005. Soluble bio-markers in vascular disease: much more than gauges of disease? Clin. Exp. Pharmacol. Physiol. 32, 233–240.

Wu, L., Iwai, M., Nakagami, H., Li, Z., Chen, R., Suzuki, J., Akishita, M., de Gasparo, M., Horiuchi, M., 2001. Roles of angiotensin II type 2 receptor stimulation associated with selective

angiotensin II type 1 receptor blockade with valsartan in the improvement of inflammation-induced vascular injury Circulation 104, 2716–2721.

Yusuf, S., Diener, H.C., Sacco, R.L., Cotton, D., Ounpuu, S., Lawton, W.A., Palesch, Y., Martin, R.H., Albers, G.W., Bath, P., Bornstein, N., Chan, B.P., Chen, S.T., Cunha, L., Dahlof, B., De Keyser, J., Donnan, G.A., Estol, C., Gorelick, P., Gu, V., Hermansson, K., Hilbrich, L., Kaste, M., Lu, C., Machnig, T., Pais, P., Roberts, R., Skvortsova, V., Teal, P., Toni, D., VanderMaelen, C., Voigt, T., Weber, M., Yoon, B.W., 2008. Telmisartan to prevent recurrent stroke and cardiovascular events. N. Engl. J. Med. 359, 1225–1237.

Journal of Neuroscience Research

Journal of Neuroscience Research 88:2385–2397 (2010)

Immunodeficiency Reduces Neural Stem/Progenitor Cell Apoptosis and Enhances Neurogenesis in the Cerebral Cortex After Stroke

Orie Saino,[1] Akihiko Taguchi,[2] Takayuki Nakagomi,[1] Akiko Nakano-Doi,[1] Shin-ichiro Kashiwamura,[1] Nobutaka Doe,[1] Nami Nakagomi,[1] Toshihiro Soma,[3] Hiroo Yoshikawa,[3] David M. Stern,[4] Haruki Okamura,[1] and Tomohiro Matsuyama[1]*

[1]Institute for Advanced Medical Sciences, Hyogo College of Medicine, Hyogo, Japan
[2]Department of Cerebrovascular Disease, National Cardiovascular Center, Osaka, Japan
[3]Department of Internal Medicine, Hyogo College of Medicine, Hyogo, Japan
[4]VPHA and Dean's Office, College of Medicine, University of Cincinnati, Cincinnati, Ohio

Acute inflammation in the poststroke period exacerbates neuronal damage and stimulates reparative mechanisms, including neurogenesis. However, only a small fraction of neural stem/progenitor cells survives. In this report, by using a highly reproducible model of cortical infarction in SCID mice, we examined the effects of immunodeficiency on reduction of brain injury, survival of neural stem/progenitor cells, and functional recovery. Subsequently, the contribution of T lymphocytes to neurogenesis was evaluated in mice depleted for each subset of T lymphocyte. SCID mice revealed the reduced apoptosis and enhanced proliferation of neural stem/progenitor cells induced by cerebral cortex after stroke compared with the immunocompetent wild-type mice. Removal of T lymphocytes, especially the $CD4^+$ T-cell population, enhanced generation of neural stem/progenitor cells, followed by accelerated functional recovery. In contrast, removal of $CD25^+$ T cells, a cell population including regulatory T lymphocytes, impaired functional recovery through, at least in part, suppression of neurogenesis. Our findings demonstrate a key role of T lymphocytes in regulation of poststroke neurogenesis and indicate a potential novel strategy for cell therapy in repair of the central nervous system.

Key words: adult stem cells; apoptosis; cerebral cortex; ischemia; inflammation; lymphocyte; neural stem cells; $CD4^+$ T cell

Cerebral infarction causes massive neuronal cell death, followed by acute inflammation that exacerbates neuronal damage. Control of poststroke inflammation is a crucial factor underlying functional recovery (Yilmaz et al., 2006; Hurn et al., 2007; Popovich and Longbrake, 2008). Although accumulation and activation of macrophages and granulocytes has been a focus of studies assessing the inflammatory response in stroke, increasing evidence points to an important role of T lymphocytes in regulating poststroke inflammation (Hurn et al., 2007; Liesz et al., 2009). The inflammatory response after stroke is also known to trigger reparative mechanisms, including activation of neurogenesis. However, such insult-induced neurogenesis is quite inefficient, in that most of the newly generated neural stem cells do not survive (Arvidsson et al., 2002). In view of the close temporal relationship between neurogenesis and inflammation in the poststroke brain, a mechanistic understanding of the interaction of these events certainly seems relevant. In particular, an important question concerns the possible relationship between inflammatory and/or other environmental factors and survival of neural stem cells developed in poststroke brain.

In this context, analysis of immunocompromised patients, achieved by T-lymphocyte suppression, revealed that transplanted bone marrow cells differentiated into multiple mature cell types, including neurons

The first three authors contributed equally to this work.

Contract grant sponsor: Grant-in-Aid for Scientific Research JSPS KAKENHI; Contract grant number: 18234567; Contract grant sponsor: Hyogo College of Medicine (2009); Contract grant sponsor: Mitsubishi Pharma Research Foundation (2009); Contract grant sponsor: Takeda Science Foundation (2005).

*Correspondence to: Prof. Tomohiro Matsuyama, MD, PhD, Institute for Advanced Medical Sciences, Hyogo College of Medicine, 1-1 Mukogawacho, Nishinomiya, Hyogo, Japan, 663-8501.
E-mail: tomohiro@hyo-med.ac.jp

Received 31 October 2009; Revised 16 February 2010; Accepted 9 March 2010

Published online 21 April 2010 in Wiley InterScience (www.interscience.wiley.com). DOI: 10.1002/jnr.22410

(Mezey et al., 2003). This finding suggests links between the immune system and survival of neural stem cells.

Insult-induced neurogenesis follows a specific sequence of events, such as the activation of adult neural stem cells, proliferation of transit-amplifying progenitor cells, migration of neuroblasts, and survival and maturation of the newborn neurons (Okano and Sawamoto, 2008), although the details are still unknown. We recently have detected and isolated the neural stem/progenitor cells that express nestin and differentiate into neurons from post-stroke cerebral cortex in mice (Nakagomi et al., 2009). Here, by using the same murine model of cerebral infarction, we demonstrate that immunodeficiency reduces apoptotic cell death of neural stem/progenitor cells after ischemic injury, resulting in the enhancement of post-stroke neurogenesis. Our results suggest a novel therapy, transiently targeting $CD4^+$ T lymphocytes, that has the potential to facilitate repair of the central nervous system (CNS) by expanding an autologous population of neural stem/progenitor cells after brain injury.

MATERIALS AND METHODS

All procedures were carried out under the auspices of the Animal Care and Use Committee of Hyogo College of Medicine and National Cardiovascular Center and in accordance with the criteria outlined in the *Guide for the care and use of laboratory animals* prepared by the National Academy of Science. Quantitative analyses were conducted by investigators who were blinded to the experimental protocol and identity of samples under study.

Induction of Focal Cerebral Ischemia

Male, 6-week-old, CB-17/Icr-+/+Jcl mice (CB-17 mice; Clea Japan Inc., Tokyo, Japan) and CB-17/Icr-scid/scid Jcl mice (SCID mice; Clea Japan Inc.) were used in this study. Permanent focal cerebral ischemia was produced by ligation and disconnection of the distal portion of the left middle cerebral artery (MCA) as described elsewhere (Taguchi et al., 2004, 2007). In brief, the left MCA was isolated, electrocauterized, and disconnected just distal to crossing the olfactory tract (distal M1 portion) with animals under halothane anesthesia. Cerebral blood flow (CBF) in the MCA area was monitored as described previously (Matsushita et al., 1998), and all mice showed a reduction in CBF to less than 25% of the baseline after MCA occlusion. Body temperature was maintained at 36.5–37°C with a heat lamp (Nipponkoden, Tokyo, Japan) during the operation and for 2 hr thereafter. Cerebral infarction produced in this strain is highly reproducible and limited to the ipsilateral cerebral cortex (Taguchi et al., 2004, 2007).

Immunohistochemistry

To analyze infarcted cortex histochemically, mice were deeply anaesthetized with sodium pentobarbital and perfused transcardially with 4% paraformaldehyde. Then, brains were removed, and coronal sections (14 μm) were stained with mouse antibody to nestin (Millipore, Billerica, MA; 1/200), NeuN (Millipore; 1/200); rabbit antibody to Fas (Wako, Osaka, Japan; 1/200), caspase-3 (R&D systems, Minneapolis, MN; 1/100), and CD3 (AnaSpec, San Jose, CA; 1/100); and rat antibody to CD4 (Biolegend; 1/50), CD8 (Biolegend; 1/50), and bromodeoxyuridine (BrdU; Abcam, Cambridge, United Kingdom; 1/100). As secondary antibody, Alexa Fluor 488 or Alexa Fluor 555 goat anti-mouse IgG (rabbit or rat; Invitrogen, Carlsbad, CA; 1/500) was used. Cell nuclei were stained with DAPI (Kirkegaard & Perry Laboratories, Gaithersburg, MD; 1/1,000). To investigate cell proliferation at 3 and 7 days after stroke, BrdU (Sigma-Aldrich, St. Louis, MO; 50 mg/kg) was administered 6 hr before fixation. To identify the neuronal cells generated during the period from day 3 through day 28 after stroke, BrdU was administered at day 3 and every 3 days before fixation. Tissue was pretreated with 2 N HCl for 30 min at 37°C and 0.1 M boric acid, pH 8.5, for 10 min at room temperature, then stained with antibody to BrdU. The number of nestin/BrdU or NeuN/BrdU double-positive cells at the border of infarction including infarcted and periinfarct area (0.5 mm in width) was counted under a confocal laser scanning microscope (Carl Zeiss International, Jena, Germany). To perform quantitative analysis of T cells, all CD4- or CD8-positive cells within the infarcted area were counted in brain sections obtained from CB-17 mice at 3 or 6 hr or 1, 3, or 7 days after stroke. Then, the number of positive cells for each marker was determined in a modified version of Image J (Brown et al., 2005). Results were expressed as the number of cells/mm^2. To observe the glial response after stroke, brain sections harvested at 1, 3, or 7 days after stroke were stained with rabbit polyclonal antibody to Iba-1 (Wako Pure Chemical Industries, Osaka, Japan; 1/200) or GFAP (Dako, Glostrup, Denmark; 1/800), followed by incubation with biotinylated goat anti-rabbit IgG (Millipore; 1/500) as secondary antibody. Antigens were visualized with ABC Elite reagent (Vector Laboratories, Burlingame, CA) and diaminobenzidine (DAB; Sigma) reaction.

Terminal Deoxynucleotidyl Transferase-Mediated dUTP-Biotin Nick End Labeling (TUNEL) Assay

Fresh-frozen sections were cut on a cryostat, fixed in 1% paraformaldehyde in PBS, postfixed in ethanol/acetic acid (2:1), and stained with an ApopTag Plus peroxidase In Situ Aopotosis Detection Kit (Millipore) according to the manufacturer's protocol. Slides were then counterstained with hematoxylin (Muto Pure Chemicals, Tokyo, Japan). The numbers of TUNEL-positive cells at the border of infarction (0.5 mm in width) were counted in Image J. Four representative fields of the infarcted area were photographed under light microscopy (Olympus, Tokyo, Japan) at ×400 magnification, and TUNEL-positive cells per field were counted. Six independent experiments were performed. Results are presented as the number of cells per square millimeter.

Quantification of Caspase-3 Level

The activity of caspase-3 was examined with a caspase-3 assay kit (Colorimetric Sigma) according to the manufacturer's protocol. Briefly, on day 7 after stroke, cortical tissues from the infarcted area were homogenized in lysis buffer and centrifuged at 20,000*g* for 15 min. Supernatants were mixed with assay buffer and caspase-3 substrate. Absorbance at 405 nm

was measured, and caspase-3 activity was calculated (n = 3 in each group). To investigate Fas-mediated signaling in vivo, Fas agonist (Jo-2; Becton Dickinson, Franklin Lakes, NJ; 0.4 μl, 0.5 μg/ml) was intracranially injected into cerebral cortex at the left MCA area (2.5 mm lateral from the bregma) on day 6 after stroke, and caspase-3 activity was calculated 24 hr after the injection (n = 3 in each group).

Measurement of Infarcted Volume

The brains were harvested at 6, 24, and 72 hr after stroke; sliced into five 2-mm coronal sections; and stained with 1.2% tryphenyltetrazolium chloride (TTC; Nacalai Tesque, Kyoto, Japan) in 0.1 mol/liter phosphate buffer solution. Seven days after stroke, mice were perfused transcardially with 4% paraformaldehyde, their brains were removed, and coronal sections (14 μm) were stained with Mayer's Hematoxylin and Eosin-Phloxine Solution (Hayashi Pure Chemical, Osaka, Japan; HE staining). Infarcted area was measured in Image J. Infarct volume was calculated by integrating the overall coronally oriented infarct area. When calculating cerebral infarct volume, the influence of cerebral edema was excluded by using correction formulas as described previously (Kitano et al., 2004). In brief, percentage cerebral edema was calculated as {[(volume of infracted hemisphere) − (volume of normal hemisphere)]/(volume of normal hemisphere)} × 100. Then, corrected infarct volume was calculated (actual measurement infarct volume) × [100/(100 + percentage cerebral edema)]. Then, relative infarct volume (%I) was calculated as 100 × (corrected infarct volume/volume of normal hemisphere × 2).

Measurement of Involution of Ipsilateral Cerebral Hemisphere Volume

Twenty-eight days after stroke, mice were perfused transcardially with 4% paraformaldehyde, brains were removed, and coronal sections (14 μm) were stained with mouse antibody to NeuN, followed by reaction with biotinylated goat anti-mouse IgG (Chemicon, Temecula, CA; 1/500), ABC Elite reagent (Vector Laboratories, Burlingame, CA), and DAB (Sigma) as chromogen. The area of the ipsilateral and contralateral cerebral hemisphere occupied by the neuronal nuclear marker NeuN was measured in Image J. Ipsilateral and contralateral cerebral hemisphere volume was calculated by integrating coronally oriented ipsilateral and contralateral cerebral hemisphere area. Involution of ipsilateral cerebral hemisphere volume was calculated as (ipsilateral/contralateral cerebral hemisphere volume).

Depletion of T Lymphocytes and Immunosuppression

CD4-, CD8-, and CD25-positive cells were depleted by intraperitoneal injection of rat monoclonal antibodies against CD4 (L3T4; clone RM4-5, IgG2a,κ, 2.5 mg/kg), CD8a (Ly-2; clone 53-6.7, IgG2a,κ, 5.0 mg/kg), or CD25 (p55; clone 3C7, IgG2b,κ, 5.0 mg/kg; BD Biosciences, San Jose, CA) 1 day before and 3 days after stroke. Rat IgG isotype control (IgG; Southern Biotech, Birmingham, AL; 2.5 mg/kg,) was administered as a control. Depletion of CD4-, CD8-, and CD25-positive cells was confirmed by FACS analysis of splenocytes isolated from mice on day 7 after stroke using FITC anti-CD3, PE anti-CD4, PE anti-CD8a, PE anti-CD25, and APC anti-TCR α-chain (BD Biosciences).

Behavioral Analysis

To assess cortical function, mice were analyzed by behavioral testing using the open field task 28 days after stroke, as described previously (Taguchi et al., 2004). Briefly, animals were allowed to search freely in a square acrylic box (30 × 30 cm) for 20 min. A light source on the ceiling of the enclosure was on during the first 10 min (light period) and off during a subsequent 10-min period. On the X- and Y-banks of the open field, two infrared beams were mounted 2 cm above the floor, spaced with a 10-cm intervals, forming a flip–flop circuit between them. The total number of beam crossings by the animal was counted and scored as traveling behavior (locomotion). To exclude the contribution of physical deficits directly related to the operative procedure and induction of stroke, motor deficiencies were examined at the same time point after MCA occlusion. Neurologic deficits were scored on a three-point modified scale: no neurologic deficit (0); failure to extend the left forepaw fully (1); circling to left (2); and loss of walking or righting reflex (3), as described by Taguchi et al. (2004). On day 28 after stroke, no mouse showed motor deficiency evaluated by this three-point modified scale (data not shown).

Analysis of Cytokine Levels in the Poststroke Area

On days 1 and 3 after induction of stroke, protein samples were obtained from infarct tissue, and the level of certain cytokines, including IL-1β, IL-6, IL-10, MIP-1α, MCP-1, TNF-α, and IFN-γ, was evaluated. Tissue was disrupted in the presence of PBS containing protease inhibitors (Complete, Roche, Mannheim, Germany). Cytokine levels were evaluated with Bio-Plex Mouse Cytokine Standards Group I (Bio-Plex suspension array system; Bio-Rad Laboratories, Hercules, CA) according to the manufacturer's protocol.

Statistical Analysis

Results are reported as mean ± SE. Statistical comparisons among groups were determined by ANOVA, and the Fisher's least significant difference (LSD) was used for post hoc analysis to compare with controls. Where indicated, individual comparisons were performed by Student's *t*-test. Significance was assumed at $P < 0.05$.

RESULTS

Preferential Expansion of Poststroke Cortex in SCID Mice vs. Immunocompetent Controls

Previously, we established a highly reproducible murine model of stroke and showed that therapeutic angiogenesis after stroke accelerated endogenous neurogenesis (Taguchi et al., 2004). For vehicle-treated SCID mice subjected to cerebral ischemia (a control group), we observed unexpected expansion of the residual ipsilateral cerebral cortex. To extend these findings, cerebral ischemia was induced in SCID mice and strain-matched (CB-17) wild-type (immunocompetent) controls. Serial evaluation of the infarcted area by TTC staining, which is restricted to the cerebral cortex of MCA territory, displayed

no significant difference between CB-17 and SCID mice (Fig. 1A) during the period from 6 hr through 3 days after stroke. Similar findings were obtained on day 7 after stroke (Fig. 1B). The temporal profile of infarct volume was not significantly different between CB-17 and SCID mice up to day 7 after stroke (Fig. 1C).

However, on day 28 after stroke, SCID mice but not CB-17 mice showed the expansion of residual ipsilateral hemisphere (Fig. 1D). Further analysis of the volume of each hemisphere, based on NeuN staining, demonstrated significant increase in poststroke brain volume in SCID mice compared with CB-17 mice (Fig. 1E,F).

Glial Response to Cerebral Infarction in SCID Mice

To investigate whether expansion of affected cortex in SCID mice and atrophic changes in CB-17 mice were related to the glial response, the temporal profile of the expression of astrocytes (Fig. 2A,B) and microglia (Fig. 2C,D) was examined on days 3 and 7 after stroke. GFAP-positive astrocytes at the border of infarction showed no apparent difference in number between groups on day 3 after stroke (SCID vs. CB-17). However, on day 7 after stroke, the number of GFAP-positive astrocytes appeared to be increased in SCID mice compared with CB-17 mice. Quantitative analysis confirmed the increased numbers of GFAP-positive astrocytes in SCID mice (Fig. 2B).

The distribution of microglia evaluated with anti-Iba-1 antibody (Liu et al., 1993) appeared principally confined to the border of infarction (Fig. 2C). In contrast to GFAP-positive astrocytes, no apparent difference was observed in number of activated microglia between groups (SCID vs. CB-17) even on day 7 after stroke (Fig. 2D). Because microglia are an important source of cytokines (Uno et al., 1997) in the poststroke inflammatory response, expression of certain mediators in infarcted tissue (IL-1β, IL-6, Il-10, MIP-1α, MCP-1, TNF-α, and IFN-γ) was measured (Fig. 2E). In each case, levels of these cytokines were virtually identical in SCID and CB-17 at 1 and 3 days after stroke.

Enhanced Neurogenesis in Poststroke SCID Mice

To investigate the neurogenesis in poststroke brain, the number of nestin-positive cells at the border of infarction was evaluated on days 3 and 7 after stroke (Fig. 3A). Quantitative analysis revealed significantly increased numbers of nestin-positive cells in SCID mice at both time points compared with CB-17 mice (Fig. 3B). Several studies have shown that some glial cells such as radial glia in development and specific subpopulations of astrocytes in adult mammals function as primary progenitors or neural

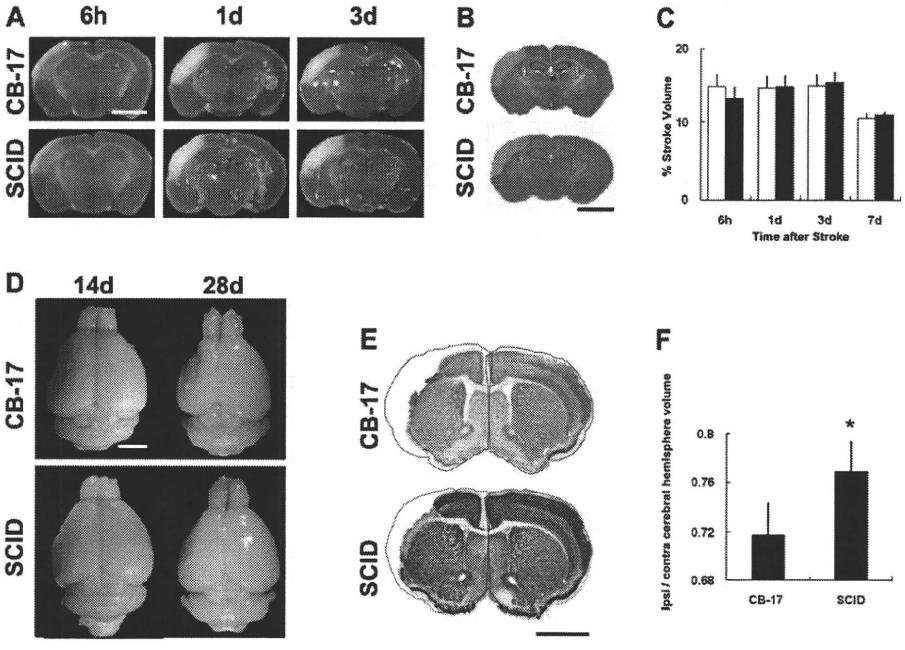

Fig. 1. Cerebral infarction in CB-17 and SCID mice. **A–C:** Evaluation with TTC (A) and HE (B) staining revealed no significant difference in infarcted size between CB-17 and SCID mice until day 7 after stroke (C; open bars, CB17; solid bars, SCID). **D–F:** Compared with day 14 after stroke, expansion of residual ipsilateral cerebral cortex was observed on day 28 in SCID mice but not in CB-17 mice (D). Analysis of stroke volume on day 28 based on analysis of NeuN staining (E) confirmed a significant difference in brain volume in the poststroke hemisphere in comparing the groups (F). In A–C, n = 5 for each experimental group; in D–F, n = 6 for each experimental group. $^*P < 0.05$ vs. CB-17 mice. Scale bars = 2 mm.

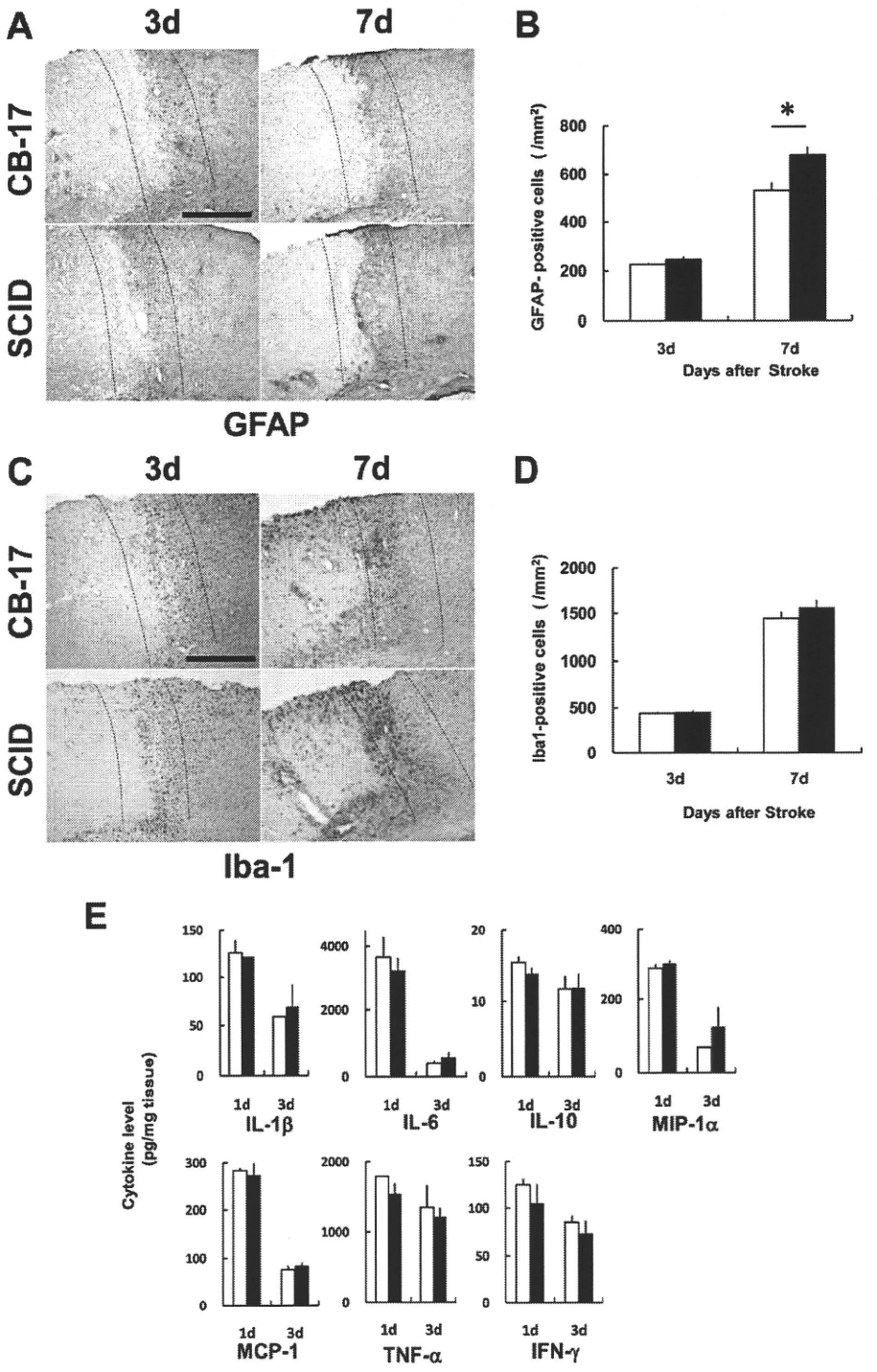

Fig. 2. Response of astrocytes and microglia in the poststroke brain. **A–D:** Expression of astrocytes (A,B) and microglia (C,D) was evaluated with anti-GFAP and anti-Iba-1 antibody, respectively. Quantitative analysis revealed increased numbers of astrocytes on day 7 after stroke in SCID mice, although no significant difference was observed on day 3, in comparing groups (B; open bars, CB-17; solid bars, SCID). In contrast, the number of microglia was not different between groups from day 3 through day 7 after stroke (D; open bars, CB17; solid bars, SCID). **E:** The level of inflammatory cytokines in the infarcted tissue on days 1 and 3 after stroke was not significantly different between CB-17 and SCID mice (open bars, CB-17; solid bars, SCID). In A–D, n = 6 for each experimental group; in E, n = 3 for each experimental group. $^*P < 0.05$ vs. CB-17 mice. Areas indicated by dashed lines represent the border of infarction (0.5 mm in width; A,C). Scale bars = 500 μm.

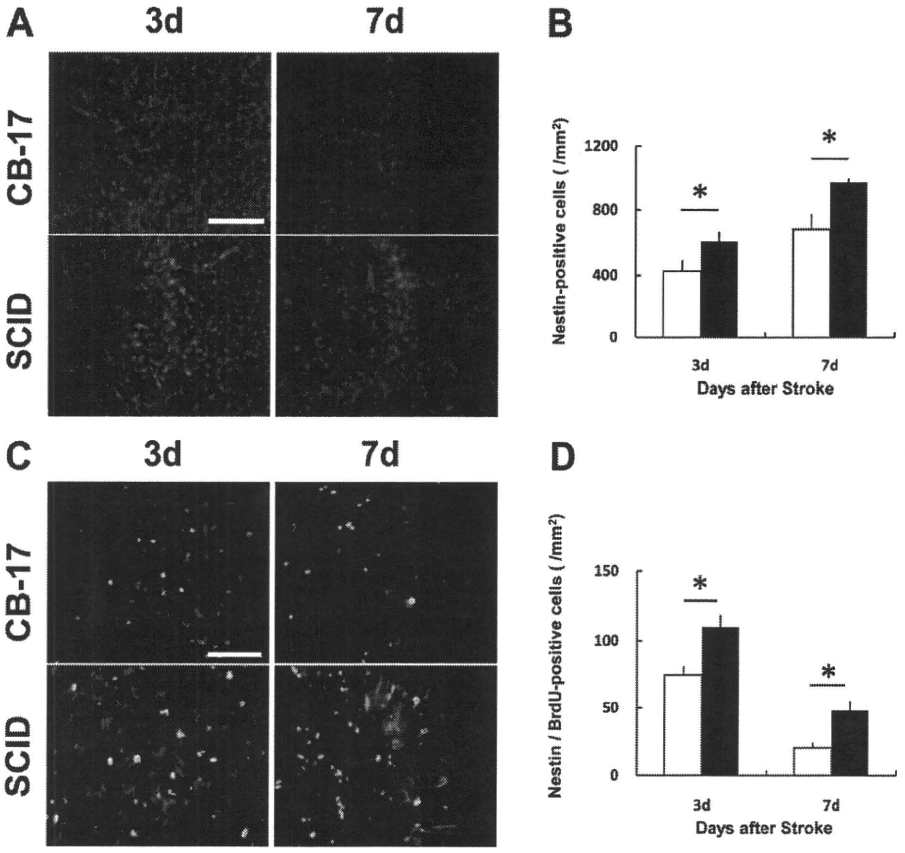

Fig. 3. Enhanced neurogenesis in poststroke SCID mice. The presence and proliferation of neural stem/progenitor cells at the border of infarction were evaluated with anti-nestin antibody (**A**; red, nestin; nuclei were counterstained with DAPI, blue), anti-nestin (red) and anti-BrdU (green) antibodies (**C**). Quantitative analysis confirmed increased number of nestin-positive (**B**) and nestin/BrdU-positive (**D**) cells in SCID mice on days 3 and 7 after stroke compared with CB-17 mice (open bars, CB-17; solid bars, SCID). In B,D, n = 6 for each experimental group. *$P < 0.05$ vs. CB-17 mice. Scale bars = 200 μm.

stem cells and express astroglial markers, including GFAP (Kriegstein and Alvarez-Buylla, 2009). Therefore, we examined the capacity for the proliferation of nestin-positive cells, which is one of the characteristics of stem cells, by combination with BrdU staining and calculated the number of nestin/BrdU-positive cells as an index of expressed neural stem/progenitor cells (Fig. 3C). Proliferation of nestin-positive cells was significantly increased in SCID mice compared with CB-17 mice (Fig. 3D). These results indicated that immunodeficiency has a significant impact on cortical expansion in poststroke mice, at least in part through accelerated proliferation of nestin-positive neural stem/progenitor cells.

Reduction of Apoptotic Cell Death in Stroke-Affected Cortex of SCID Mice

To evaluate the balance between regenerative and degenerative processes in chronic features of poststroke cortex, apoptotic cell death at the border of infarction was investigated (Fig. 4A). DNA fragmentation was studied by TUNEL staining (Fig. 4B). From day 1 to day 7 after stroke, numbers of TUNEL-positive cells gradually increased in both CB-17 and SCID mice (Fig. 4C). However, the total number of TUNEL-positive cells was significantly less in SCID mice on both day 3 and day 7 after stroke compared with CB-17 mice.

To assess apoptosis in the population of neural stem/progenitor cells, double immunostaining was performed to detect cells positive for both nestin and caspase-3. On day 3 after stroke, few caspase-3-positive cells were observed in SCID mice (Fig. 4D, green, nestin; red, caspase-3), whereas CB-17 mice appeared to have abundant nestin/caspase-3 double-positive cells (Fig. 4E,F, green, nestin; red, caspase-3) inside and at the border of the infarction. Consistently with these immunohistochemical data, the level of caspase-3 activity in tissues from the infarction was lower in SCID than CB-17 mice (Fig. 4G). These results suggested that apoptotic cell death was suppressed in SCID mice. To identify a possible trigger of caspase-3 activation in nestin-

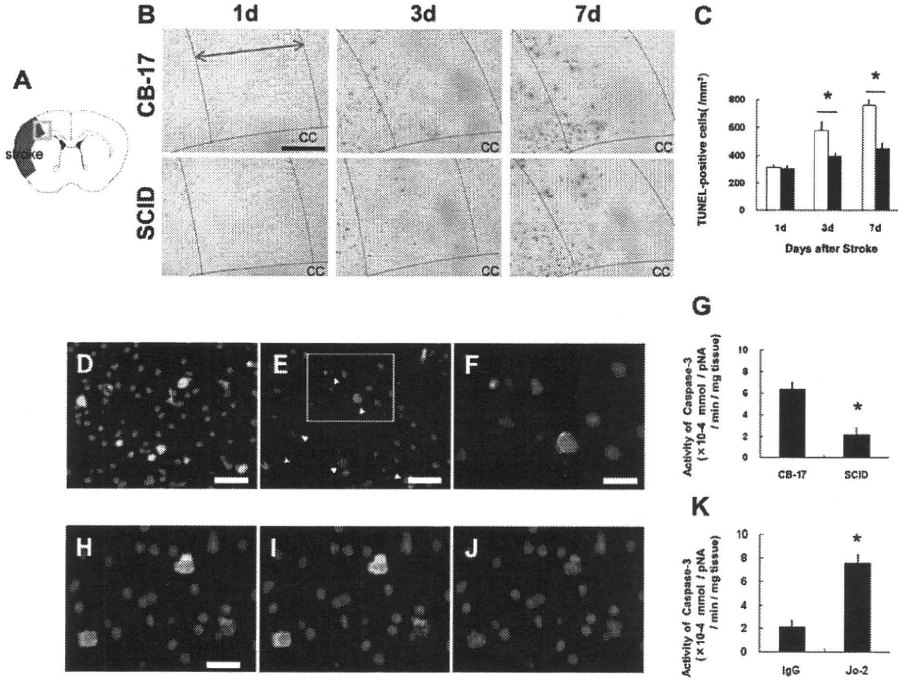

Fig. 4. Reduction in apoptotic neural stem/progenitor cell death in SCID mice. **A–C:** Apoptotic cell death at the border of infarction (A) was investigated with TUNEL staining on days 1, 3, and 7 after stroke (B). Although no significant difference in the number of TUNEL-positive cells was observed on day 1 after stroke, a significant reduction in the number of apoptotic cells was observed in SCID mice on days 3 and 7 after stroke compared with CB-17 mice (C; open bars, CB17; solid bars, SCID). **D–F:** Coexpression of nestin (green) and caspase-3 (red) was investigated 3 days after stroke. Few cells coexpressing both markers were observed in SCID mice (D), whereas most of the nestin-positive cells (arrowheads) in CB-17 mice expressed caspase-3 at the same time (E, lower magnification; F, higher magnification). **G:** The level of caspase-3 activity in the infarcted tissue was significantly increased in CB-17 mice compared with SCID mice. **H–J:** Coexpression of nestin and Fas was observed in cells located in the infarcted area in SCID mice on day 3 after stroke (H, merged image; I, nestin; J, Fas). **K:** Intracerebral injection of Jo-2 increased caspase-3 activity in SCID mice in vivo. In C, n = 6; in G,K, n = 3 for each experimental group. $^*P < 0.05$ vs. CB-17 mice. Areas indicated by dashed lines represent the border of infarction (0.5 mm in width; B), and solid lines indicate the border to corpus callosum (cc in B). Scale bars = 200 μm in B; 50 μm in D,E; 20 μm in F–J.

positive cells, Fas-mediated signalling (Niho and Asano, 1998; Mannick et al., 1999) was investigated in the poststroke cortex of SCID mice on day 3. Double immunostaining for Fas and caspase-3 demonstrated the expression of Fas in nestin-positive cells [Fig. 4H, merged image (green, nestin; red, Fas); 4I, nestin; 4J, Fas].

To confirm the in vivo activation of Fas-mediated signalling in neural stem/progenitor cells, Jo-2 (an Fas agonist antibody) was injected into the infarcted cortex of poststroke SCID mice on day 6. Increased caspase-3 activity was detected in the infarcted cortical tissue 24 hr after the injection (Fig. 4K). These results suggested that apoptosis of nestin-positive neural stem/progenitor cells in poststroke cerebral cortex was suppressed in SCID mice. Thus, a combination of increased proliferation and decreased apoptosis, occurring, at least in part, in the nestin-positive cell population, is likely to be contributing to cortical expansion in the immunocomprised mice (Fig. 1).

Depletion of T Lymphocytes, Especially CD4 T Cells, Enhances Neural Stem/Progenitor Cells Proliferation While Reducing Their Apoptosis

Next we investigated the possible role of T lymphocytes in the survival/death of neural stem/progenitors generated after ischemic insult, because T lymphocytes have been shown to contribute to neuroprotection/injury after acute stroke (Yilmaz et al., 2006; Hurn et al., 2007; Liesz et al., 2009). Immunocytochemistry for CD4 and CD8 in CB-17 mice showed virtually no CD4- or CD8-positive cells in the cerebral cortex prior to induction of stroke (not shown). After stroke, CD4-positive T cells were detected in the infarcted area

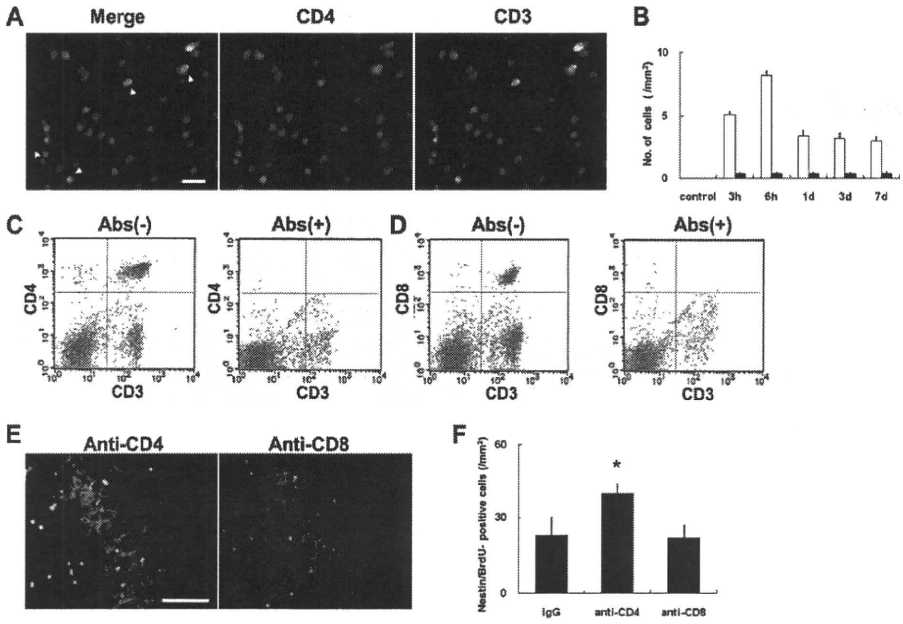

Fig. 5. Depletion of CD4-positive T lymphocytes enhances neurogenesis in poststroke brain. **A,B:** Infiltration of CD4-positive T cells (A, arrowhead) was observed in CB-17 mice on day 3 after stroke (red, CD4; green, CD3; nuclei were counterstained with DAPI [blue]). In contrast, infiltration of CD8-positive cells was rarely observed (not shown). Cells expressing CD4 (white bars) or CD8 (darkened bars) in the infarcted area and sham operated cortex were quantified at 3 and 6 hr and 1, 3, and 7 days after stroke (B). **C,D:** Depletion of CD4 (C) and/or CD8 (D) T cells was confirmed by FACS of splenocytes from mice treated with each antibody. **E,F:** Immunohistochemical analysis for nestin (red)-/BrdU (green)-positive cells was performed in the sections from mice treated with anti-CD4 or anti-CD8 antibody on day 7 after stroke (E). Quantitative analysis revealed that removal CD4-positive T cells, but not CD8-positive cells, increased the number of nestin/BrdU-positive cells at the border of infarction compared with control (F). In B, n = 4; in F, n = 7 for each experimental group. $*P < 0.05$ vs. control IgG group. Scale bars = 50 μm in A; 100 μm in E.

(Fig. 5A; red, CD4; green, CD3). In contrast, CD8-positive cells were rarely observed (not shown). The number of CD4- and CD8-positive cells was quantified in relation to induction of stroke; infiltration of CD4-positive cells into the infarct cortex was observed within 3 hr of stroke (Fig. 5B). In contrast, no CD4- or CD8-positive cells were observed in nonischemic cortex, including the contralateral side (not shown).

To investigate whether T lymphocytes could contribute to neural stem/progenitor cell death after stroke in vivo, selective depletion of T lymphocytes from CB-17 mice was achieved by administering antibodies to either CD4 or CD8 antibody 1 day before and 3 days after stroke. Depletion of CD4- or CD8-positive lymphocytes was confirmed by FACS analysis of the splenocytes from the poststroke mice (Fig. 5C,D). Seven days after stroke, animals subjected to depletion of CD4 T cells displayed significantly increased numbers of nestin/BrdU double-positive cells in the periinfarct area, although no significant effect was observed on depletion of CD8-positive cells (Fig. 5E,F). Coincidentally, animals depleted for CD4 T cells showed significantly decreased number of nestin/caspase-3 double-positive cells in the periinfarct area compared with the control IgG-treated mice (Fig. 6A–I). Caspase-3 activity evaluated in tissues from the infarction on 7 days after stroke was reduced following depletion of CD4-positive cells (Fig. 6J). These results suggested that depletion of CD4-positive T lymphocytes suppressed apoptotic cell death of nestin-positive neural stem/progenitors in poststroke cerebral cortex.

Enhanced Endogenous Neurogenesis on Depletion of CD4-Positive T Lymphocytes

To provide further support for our hypothesis that lymphocytes participate in the neurogenesis after stroke, proliferated neuronal cells were investigated in poststroke CB-17 mice following depletion of T lymphocyte. On day 28 after stroke, multiple NeuN/BrdU double-positive cells were observed at the border of infarction, including thec periinfarct area, following depletion of CD4-positive cells, although fewer NeuN/BrdU double-positive cells were observed in mice treated with control IgG or anti-CD8 antibody (Fig. 7A; green, BrdU; red, NeuN: upper